# CONCENTRAZIONI BACKGROUND NATURALI E CONTAMINAZIONI INDICATIVE DI CONTAMINAZIONE

Con il termine background (tenore di fondo) si deve intendere la concentrazione naturale nei terreni di elementi, ivi compresa la presenza di mineralizzazioni.

Con il termine baseline (tenore di fondo attuale) si deve intendere la concentrazione di elementi misurata in un certo sito attualmente, comprendendo quindi anche la presenza nei terreni di elementi di origine antropica.

Nel passato sono stati considerati come valori di background i valori medi crostali. Questo non è compatibile con la geochimica ambientale data la grande variazione nella composizione dei litotipi della crosta superiore.

Valutazione statistica dei valori background e/o baseline

La statistica si utilizza per discriminare i valori naturali del background rispetto ai valori contaminati di metalli nei diversi mezzi dell'ambiente.

Prima di fissare i valori di background si studiano i dati delle concentrazioni di un determinato elemento attraverso la costruzione di istogrammi di frequenza per verificare il tipo di distribuzione e se sono rappresentativi di una o più popolazioni. La statistica classica assume che una sola popolazione di dati presenta un istogramma con una distribuzione normale o gaussiana.

In questo caso, il valore background generalmente si fissa in corrispondenza della media aritmetica più una deviazione standard. La deviazione standard o scarto tipo o scarto quadratico medio è un indice di dispersione (vale a dire una misura di variabilità di una popolazione o di una variabile casuale) derivato direttamente dalla varianza, ha la stessa unità di misura dei valori osservati (mentre la varianza ha come unità di misura il quadrato dell'unità di misura dei valori di riferimento). La deviazione standard misura la dispersione dei dati intorno al valore atteso.

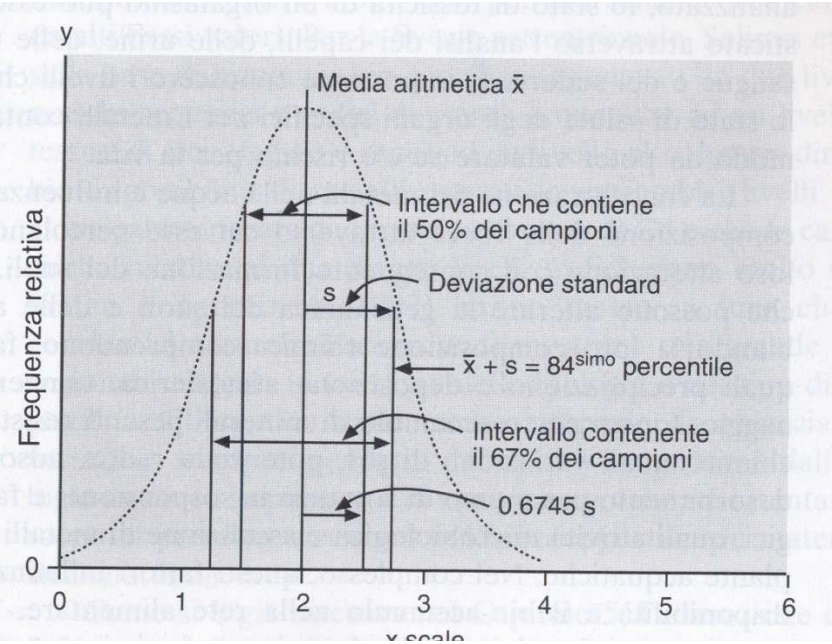

Questo metodo non è generalmente applicabile in quanto la maggior parte delle concentrazioni di metalli non hanno una distribuzione normale ma mostrano istogrammi di frequenza con una marcata coda positiva.

Skewness. Caratterizza il grado di asimmetria di una distribuzione intorno alla propria media. Una skewness positiva indica l'orientamento verso i valori positivi (parte destra), mentre una skewness negativa verso i valori negativi (parte sinistra).

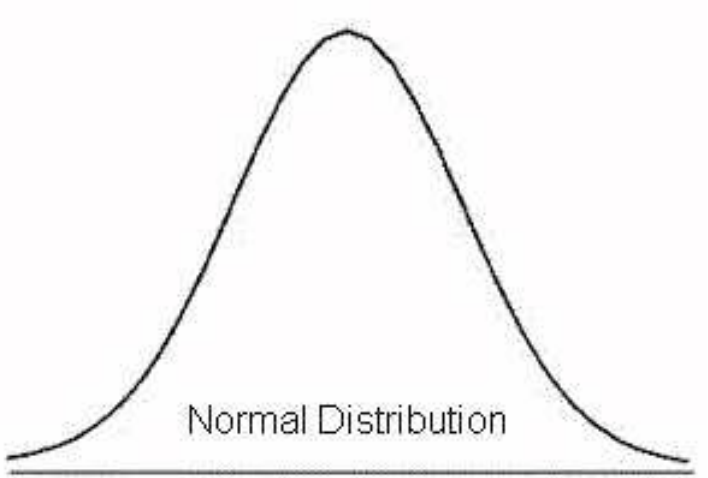


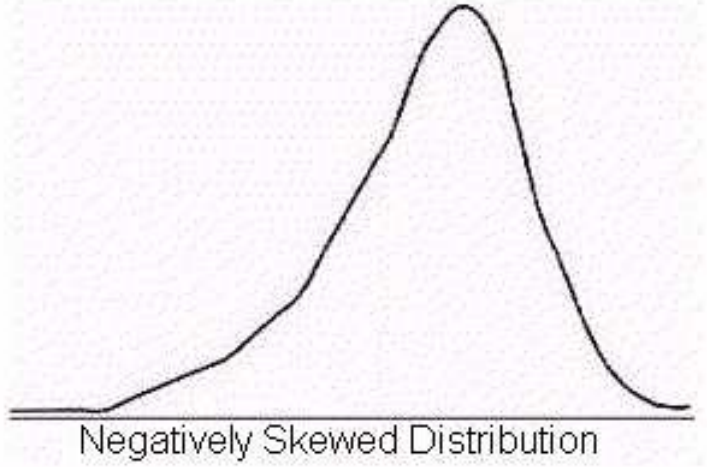


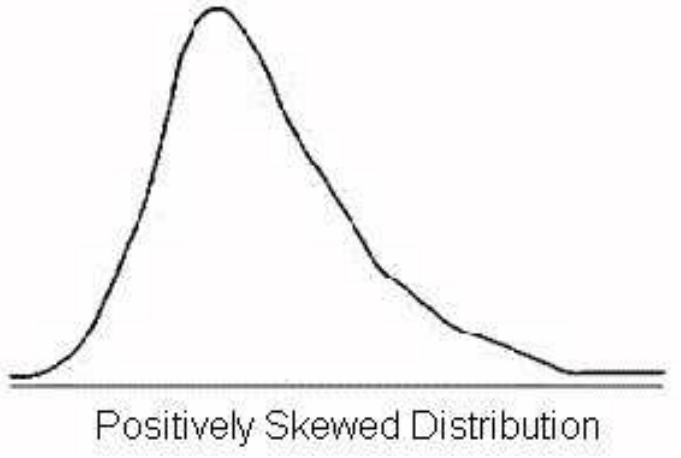

La curtosi (nota anche come kurtosis), nel linguaggio della satistica, è un allontanamento dalla normalità distributiva, rispetto alla quale si verifica un maggiore appiattimento (distribuzione platicurtica) o un maggiore allungamento (distribuzione leptocurtica).

Se il coefficiente di curtosi è:

- > 0 la curva si definisce leptocurtica, cioè più "appuntita" di una normale.
- < 0 la curva si definisce platicurtica, cioè più "piatta" di una normale.
- = 0 la curva si definisce normocurtica, cioè "piatta" come una normale.

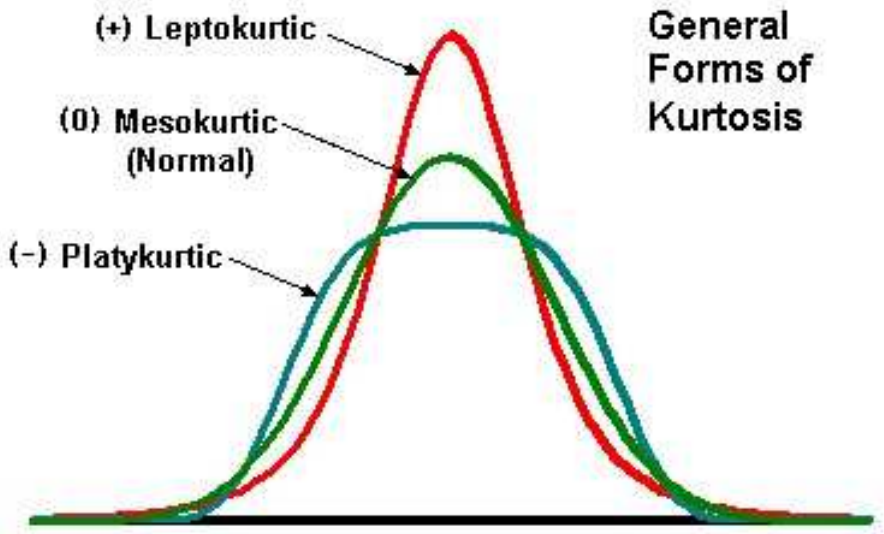

La distribuzione dei dati, soprattutto per gli elementi in traccia, tende ad essere di tipo log-normale (cioè i logaritmi dei valori delle concentrazioni sono distribuiti approssimativamente in modo normale).

In geochimica la log-normalità viene rappresentata ponendo i dati su curve cumulative di frequenza in un diagramma bilogaritmico. Se il diagramma che si ottiene è una retta significa che si è in presenza di una sola popolazione di dati. In questo caso il parametro di riferimento per il calcolo della concentrazione background della popolazione dei dati è la media geometrica.

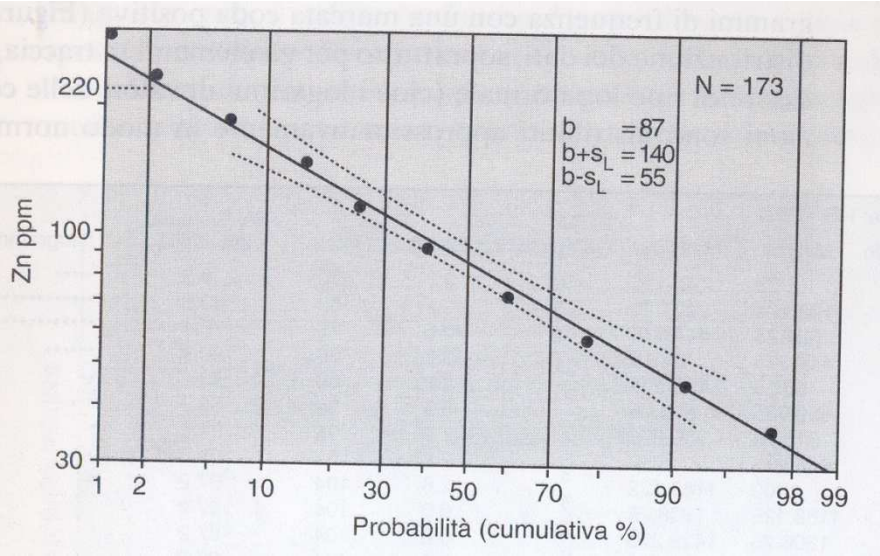


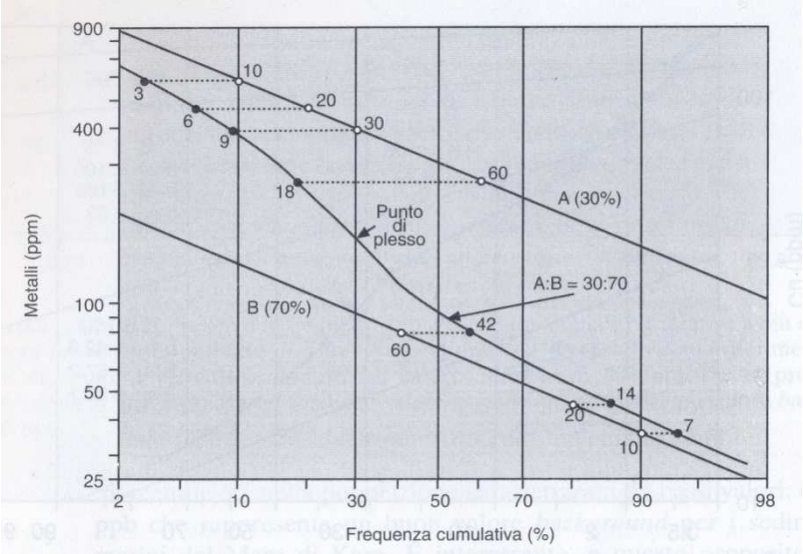

Il coefficiente di variazione è un indice di dispersione che permette di confrontare misure di fenomeni riferite a unità di misura differenti, in quanto si tratta di un numero puro (ovvero non riferito ad alcuna unità di misura).

Viene definito, per un dato campione, come il rapporto tra la sua deviazione standard (σ) e il valore assoluto della sua media aritmetica (μ):

$$CV = \frac{\sigma}{|\mu|}$$

Per un campione con un numero finito n di esemplari è dato dall'espressione

$$\sqrt{\frac{1}{n}\sum_{i=1}^{n}\left(\frac{x_i}{|\mu|} - 1\right)^2}$$

Permette di valutare la dispersione dei valori attorno alla media indipendentemente dall'unità di misura. Ad esempio, la deviazione standard di un campione di redditi espressi in Lire è completamente diversa della deviazione standard degli stessi redditi espressi in Euro, mentre il coefficiente di dispersione è lo stesso in entrambi i casi.

Analisi cluster. Evidenzia fra le variabili misurate le associazioni di elementi che consentono una più completa comprensione dei processi fisici, biologici e geochimici che sono alla base della presenza di un'associazione chimica all'interno di un determinato campione. Negli studi geochimica ambientale, l'analisi cluster viene utilizzata per inquadrare gli elementi, i minerali e i dati in gruppi più o meno omogenei (communality) in modo da evidenziare le relazioni che esistono fra i gruppi. Il raggruppamento gerarchico unisce fra di loro le osservazioni più simili.

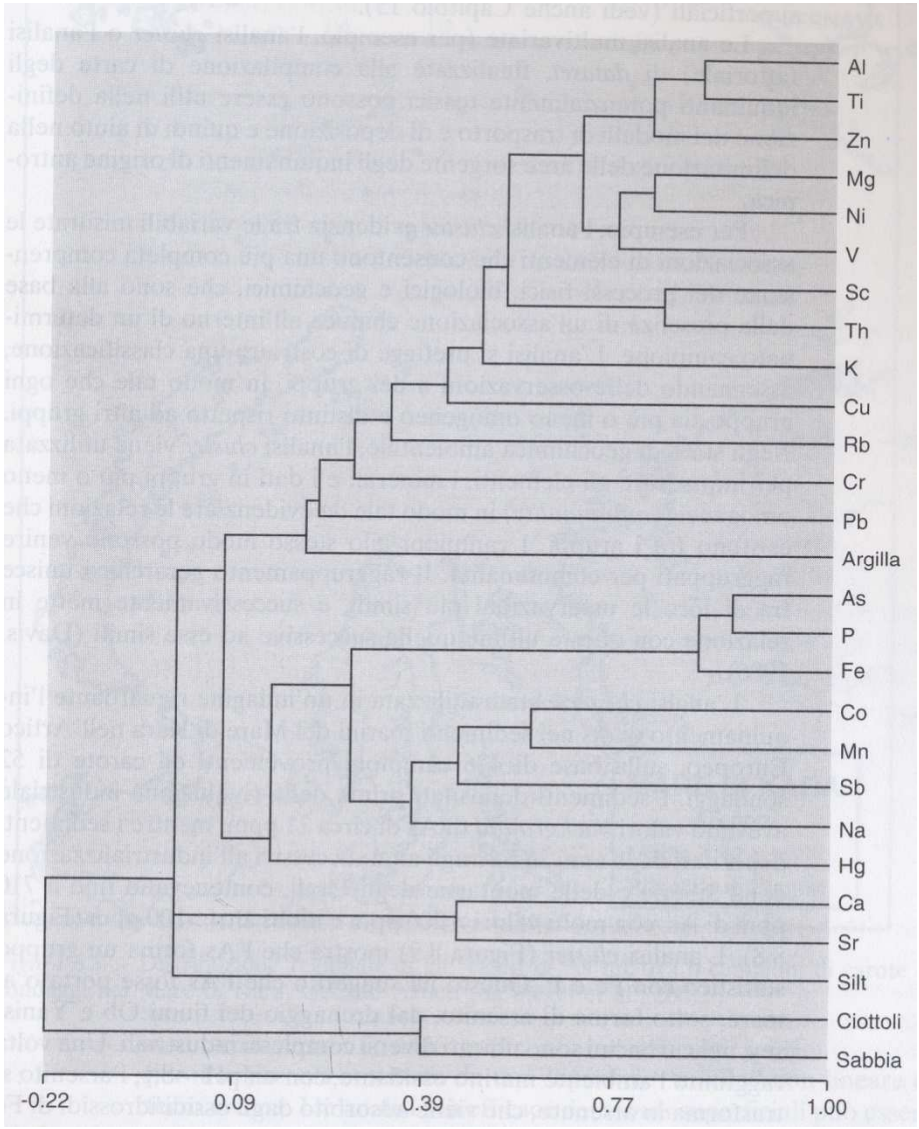

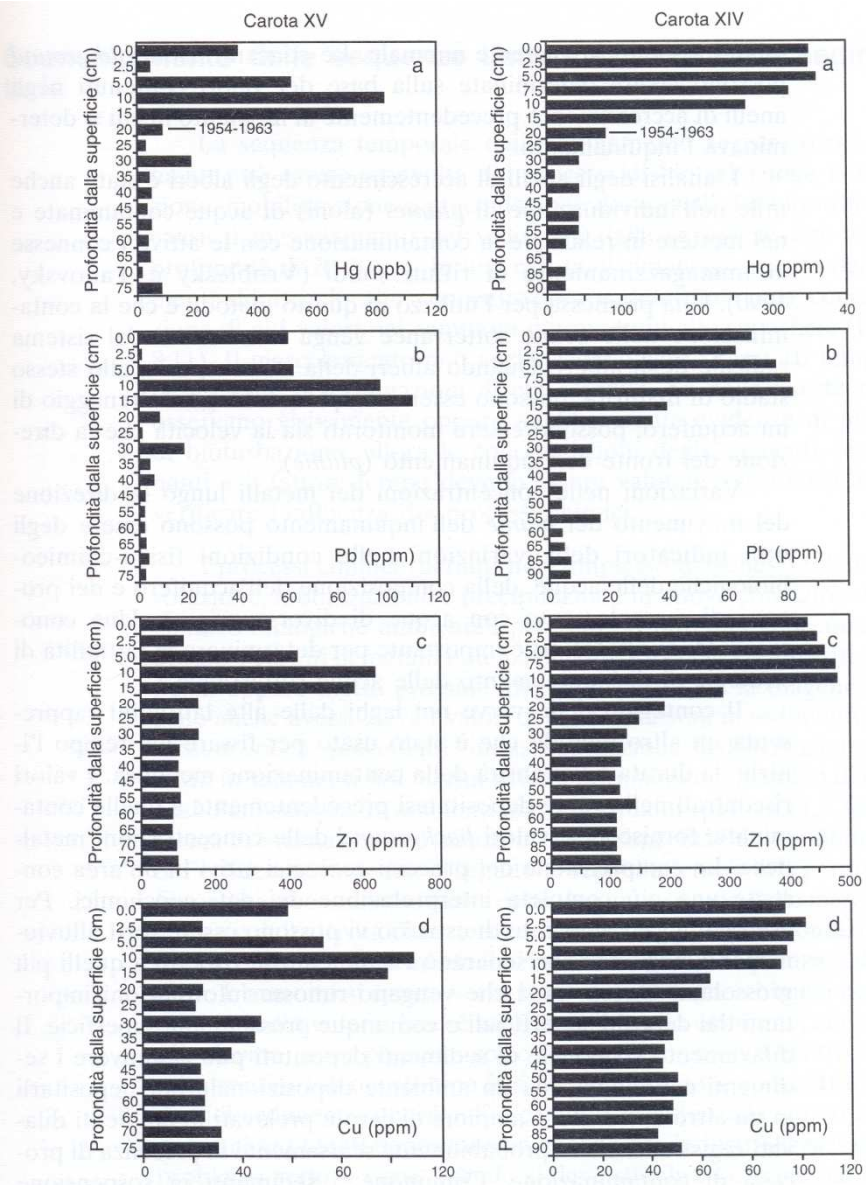


*Figura 8.10.* – Distribuzione di Hg, Pb, Zn in due carote provenienti dalla laguna di Manzalah, delta del Nilo (da Siegel et al., 1994, modificata). La carota XV è prossima alla foce di un drenaggio che trasporta acque di scarico industriali e la carota XIV è ubicata a 2 km di distanza lungo il flusso della corrente. Il ritrovamento di $^{137}Cs$ si correla bene con la chiusura della Diga Superiore di Assuan, quando si è avuto un notevole incremento dello sviluppo industriale e quindi di relativi scarichi industriali nel sistema di drenaggio fluviale. Le concentrazioni di elementi metallici decadono in modo significativo lungo il flusso correntizio.

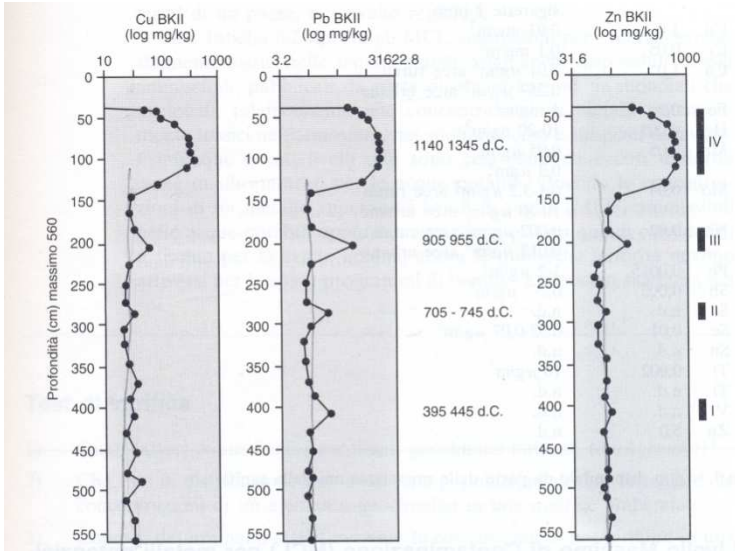


*Figura 8.12.* – Distribuzione di Cu, Pb e Zn di una carota di sedimenti alluvionali (*overbank*) proveniente da un'area delle Harz Mountains, Germania. Quattro periodi di attività mineraria vengono riflessi dalle alte concentrazioni di metalli nei sedimenti. I contenuti naturali (*bakground*) possono essere ricavati in base alle concentrazioni riscontrate nei livelli dei sedimenti più profondi rispetto al periodo più vecchio di attività mineraria (Matschullat et al., 1997, modificata).

*Tabella 8.2.* – Livelli massimi di contaminazione ammissibili per metalli potenzialmente tossici nelle acque potabili. Compilato sulla base di concentrazioni ammissibili pubblicate da diverse organizzazioni quali WHO, EPA, EC e altre. Per alcuni metalli sono riportate le concentrazioni ammissibili per l'aria.

| | Acqua mg/l | Aria |
|---|---|---|
| As | 0,05 | 0,01 $\mu g/m^3$ |
| Be | 0,004 | 0,01 $\mu g/m^3$/mese |
| Cd | 0,003 | 1-5 $ng/m^3$ aree rurali |
| | | 10-20 $ng/m^3$ aree urbane |
| | | sigarette 1 ppm |
| Co | 1,0 | 0,01 $mg/m^3$ |
| Cr | 0,05 | 0,1 $mg/m^3$ |
| Cu | 1,0 | 0,01 $\mu g/m^3$ aree rurali |
| | | 0,257 $\mu g/m^3$ aree urbane |
| Fe | 0,2 | 6 $mg/m^3$ |
| Hg | 0,001 | 10-20 $ng/m^3$ |
| Mn | 0,05 | 0,05 $\mu g/m^3$ |
| | | 0,3 $\mu gm^3$ |
| Mo | 0,04 | 0,1-3,2 $\mu g/m^3$ aree rurali |
| | | 10-30 $\mu g/m^3$ aree urbane |
| Ni | 0,02 | 0,002 $\mu g/m^3$ aree rurali |
| | | 0,015 $\mu g/m^3$ aree urbane |
| Pb | 0,0015 | 1-2 $\mu g/m^3$ |
| Sb | 0,005 | 0,2-2 $\mu g/m^3$ |
| Sc | n.d. | n.d. |
| Se | 0,01 | 0,02-0,07 $\mu g/m^3$ |
| Sn | n.d. | n.d. |
| Tl | 0,002 | 10 $\mu g/m^3$ |
| Ti | n.d. | n.d. |
| V | n.d. | n.d. |
| Zn | 5,0 | n.d. |

n.d. = non disponibile da parte delle organizzazioni della sanità.

WHO: Organizzazione Mondiale della Sanità; EPA: Agenzia per la Protezione dell'Ambiente USA; EC: Comunità Europea.

I Livelli Massimi di Concentrazione (MLC) sono stati determinati dopo indagini di laboratorio e sulla base di risultanze e osservazioni mediche relativamente all'ingestione di metalli tossici, ai loro fattori di bio-accumulo ed al loro impatto sulla salute umana.

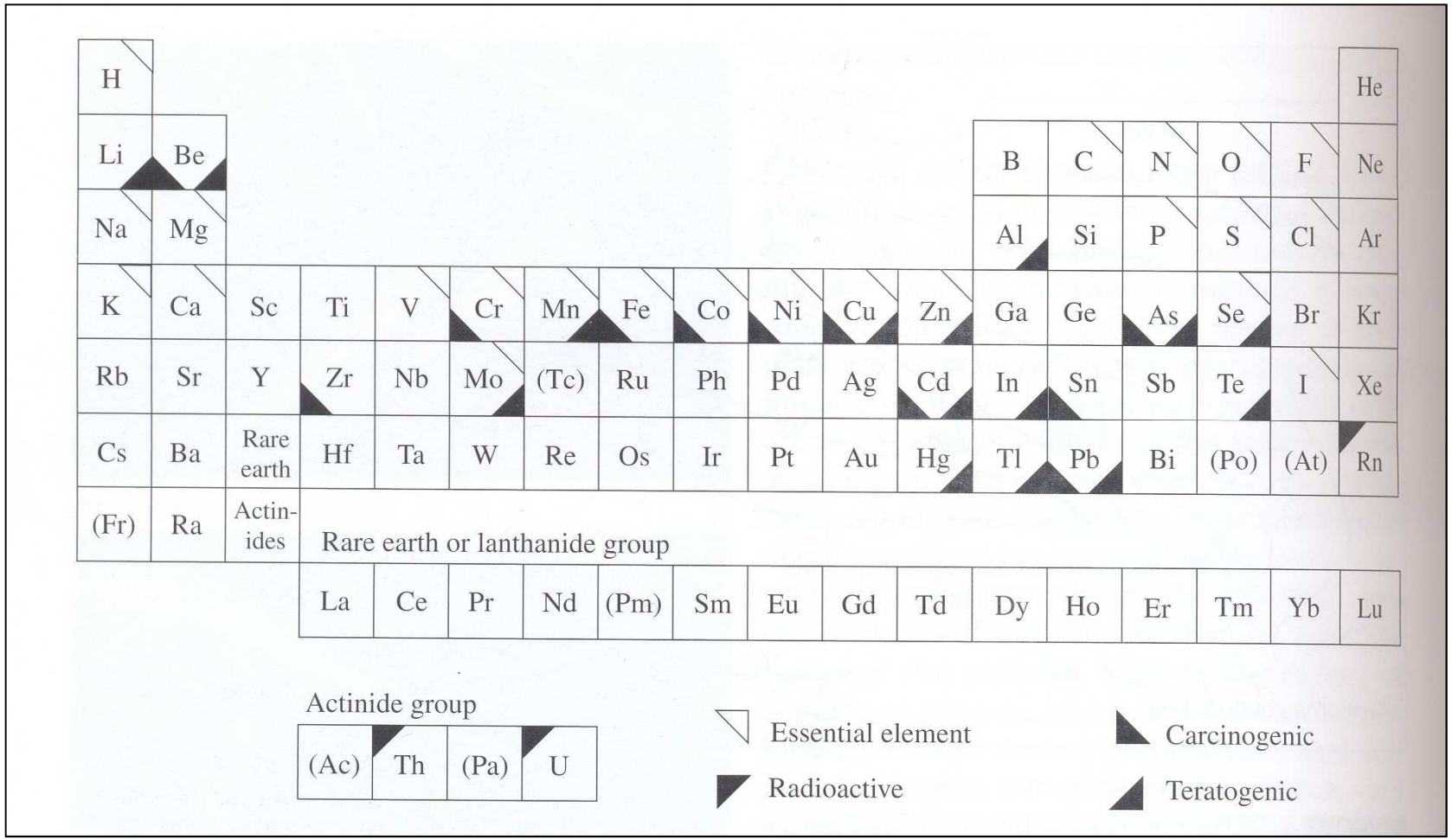


Sistema periodico degli elementi in cui vengono identificati gli elementi essenziali per la nutrizione e quelli tossici e causano cancro (carcinogenic), o difetti per i feti (teratogenic) quando ingeriti in dosi elevate.

## DECRETO LEGISLATIVO 3 aprile 2006, n. 152 *Norme in materia ambientale*

| | |
|---|---|
| -Parte Prima<br>(Artt. 1-3) | Disposizioni comuni e principi generali |
| -Parte Seconda<br>(Artt. 4-52) | Procedure per la valutazione ambientale strategica (VAS), per la valutazione dell'impatto ambientale (VIA) e per l'autorizzazione integrata ambientale (IPPC) |
| -Parte Terza<br>(Artt. 73-176) | Tutela dei corpi idrici e disciplina degli scarichi |
| -Parte Quarta<br>(Artt. 177-266) | Norme in materia di gestione dei rifiuti e di bonifica dei siti inquinati |
| -Parte Quinta<br>(Artt. 267-298) | Norme in materia di tutela dell'aria e di riduzione delle emissioni in atmosfera |
| -Parte Sesta<br>(Artt. 299-318) | Norme in materia di tutela risarcitoria contro i danni all'ambiente |

**D.Lgs. 152/06 - PARTE QUARTA**

***Norme in materia di gestione dei rifiuti e di bonifica dei siti inquinati***

Titolo I - Gestione dei rifiuti

Titolo II - Gestione degli imballaggi

Titolo III - Gestione di particolari categorie di rifiuti

Titolo IV - Tariffa per la gestione dei rifiuti urbani

Titolo V – Bonifica di siti contaminati

Titolo VI - Sistema sanzionatorio e disposizioni transitorie e finali

# D.Lgs. 152/06 - PARTE QUARTA – Art. 240 – Alcune d*efinizioni* *1/2*

*(Definizioni in parte semplificate)*

**a)** **sito:** l'area o porzione di territorio, geograficamente definita e determinata, intesa nelle diverse matrici ambientali (suolo, sottosuolo ed acque sotterranee) e comprensiva delle eventuali strutture edilizie e impiantistiche presenti;

**b)** **concentrazioni soglia di contaminazione (CSC):** i livelli di contaminazione delle matrici ambientali che costituiscono valori al di sopra dei quali e' necessaria la caratterizzazione del sito e l'analisi di rischio sito specifica

**c)** **concentrazioni soglia di rischio (CSR):** i livelli di contaminazione delle matrici ambientali, da determinare caso per caso con l'applicazione della procedura di Analisi di Rischio sito specifica (AdR) e sulla base dei risultati del piano di caratterizzazione, il cui superamento richiede la messa in sicurezza e la bonifica. I livelli di concentrazione cosi' definiti costituiscono i livelli di accettabilita' per il sito;

**d)** **sito potenzialmente contaminato:** un sito nel quale uno o più valori di concentrazione delle sostanze inquinanti rilevati nelle matrici ambientali risultino superiori alle CSC, in attesa degli esiti della caratterizzazione e della AdR, che ne permettano di determinare lo stato o meno di contaminazione sulla base delle CSR;

**e)** **sito contaminato:** un sito nel quale le CSR, determinate con l'applicazione della procedura di dell'analisi di rischio (definizione s) sulla base dei risultati del piano di caratterizzazione, risultano superati;

**f)** **sito non contaminato:** un sito nel quale la contaminazione rilevata nelle matrice ambientali risulti inferiore alle CSC oppure, se superiore risulti comunque inferiore alle CSR determinate con l'AdR

*(Definizioni in parte semplificate)*

**m) messa in sicurezza d'emergenza:** ogni intervento immediato o a breve termine, da mettere in opera in caso di eventi di contaminazione repentini di qualsiasi natura, atto a contenere la diffusione delle sorgenti primarie di contaminazione, impedirne il contatto con altre matrici presenti nel sito e a rimuoverle, in attesa di eventuali ulteriori interventi;

**o) messa in sicurezza permanente:** l'insieme degli interventi atti a isolare in modo definitivo le fonti inquinanti rispetto alle matrici ambientali circostanti e a garantire un elevato e definitivo livello di sicurezza per le persone e per l'ambiente. In tali casi devono essere previsti piani di monitoraggio e controllo e limitazioni d'uso rispetto alle previsioni degli strumenti urbanistici;

**p) bonifica:** l'insieme degli interventi atti ad eliminare le fonti di inquinamento e le sostanze inquinanti o a ridurre le concentrazioni delle stesse presenti nel suolo, nel sottosuolo e nelle acque sotterranee ad un livello uguale o inferiore alle CSR;

**q) ripristino e ripristino ambientale:** gli interventi di riqualificazione ambientale e paesaggistica, anche costituenti complemento degli interventi di bonifica o messa in sicurezza permanente, che consentono di recuperare il sito alla effettiva e definitiva fruibilità per la destinazione d'uso conforme agli strumenti urbanistici;

**s) analisi di rischio sanitario e ambientale sito specifica:** analisi sito specifica degli effetti sula salute umana derivanti dall'esposizione prolungata all'azione delle sostanze presenti nelle matrici ambientali, condotta con i criteri indicati nell'Allegato 1 alla parte quarta del presente decreto.

# Esempi di concentrazione soglia di contaminazione (CSC)

**Concentrazioni soglia di contaminazione per le acque sotterranee (D.Lgs 152/06 )**

| Sostanze | | Valori limite (µg/l) |
|---|---|---|
| **Metalli** | | |
| 1 | Alluminio | 200 |
| 2 | Antimonio | 5 |
| 3 | Argento | 10 |
| 4 | Arsenico | 10 |
| 5 | Berillio | 4 |
| 6 | Cadmio | 5 |
| 7 | Cobalto | 50 |
| 8 | Cromo totale | 50 |
| 9 | Cromo VI | 5 |
| 10 | Ferro | 200 |
| 11 | Mercurio | 1 |
| 12 | Nichel | 20 |
| 13 | Piombo | 10 |
| 14 | Rame | 1000 |
| 15 | Selenio | 10 |
| 16 | Manganese | 50 |
| 17 | Tallio | 2 |
| 18 | Zinco | 3000 |
| **Inquinanti inorganici** | | |
| 19 | Boro | 1000 |
| 20 | Cianuri liberi | 50 |
| 21 | Fluoruri | 1500 |
| 22 | Nitriti | 500 |
| 23 | Solfati (mg/litro) | 250 |

**Concentrazioni soglia di contaminazione per i terreni (D.Lgs 152/06 )**

| Sostanze | | Valori limite (mg/kg) | |
|---|---|---|---|
| **Metalli** | | **A** | **B** |
| 1 | Antimonio | 10 | 30 |
| 2 | Arsenico | 20 | 50 |
| 3 | Berillio | 2 | 10 |
| 4 | Cadmio | 2 | 15 |
| 5 | Cobalto | 20 | 250 |
| 6 | Cromo totale | 150 | 800 |
| 7 | Cromo VI | 2 | 15 |
| 8 | Mercurio | 1 | 5 |
| 9 | Nichel | 120 | 500 |
| 10 | Piombo | 100 | 1000 |
| 11 | Rame | 120 | 600 |
| 12 | Selenio | 3 | 15 |
| 13 | Stagno | 1 | 350 |
| 14 | Tallio | 1 | 10 |
| 15 | Vanadio | 90 | 250 |
| 16 | Zinco | 150 | 1500 |
| 17 | Cianuri liberi | 1 | 100 |
| 18 | Fluoruri | 100 | 2000 |

# Procedura generale

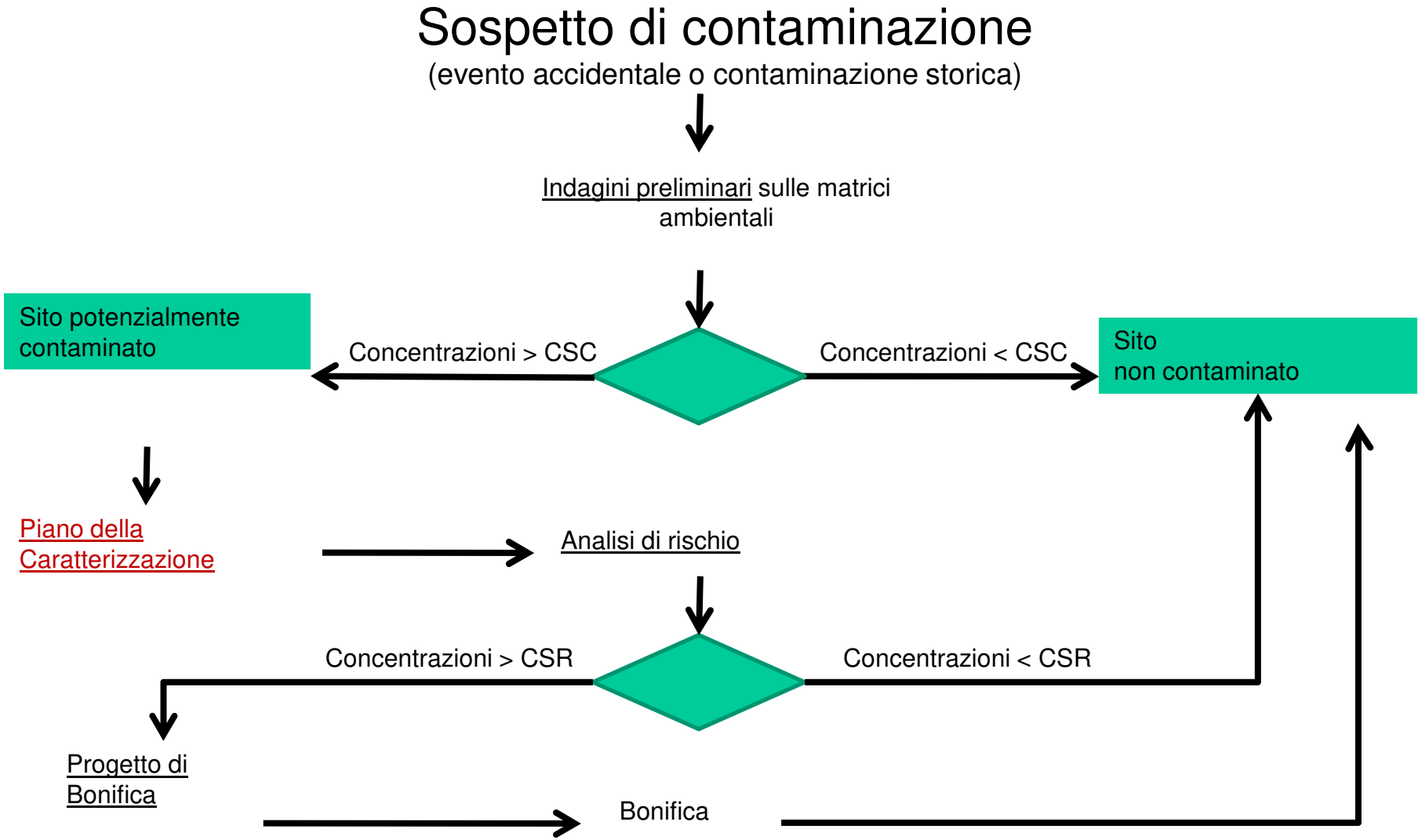

# Piano della caratterizzazione

Sulla base dei risultati delle indagini preliminari e di ulteriori indagini storiche si elabora il MODELLO CONCETTUALE PRELIMINARE del sito che permette di progettare correttamente le indagini del Piano della Caratterizzazione

Sulla base dei risultati delle indagini del Piano della Caratterizzazione si elabora il MODELLO CONCETTUALE DEFINITIVO che deve contenere tutte le informazioni relative alle componenti principali di un sito contaminato:

**Sorgente** → **Percorso** → **Recettore**

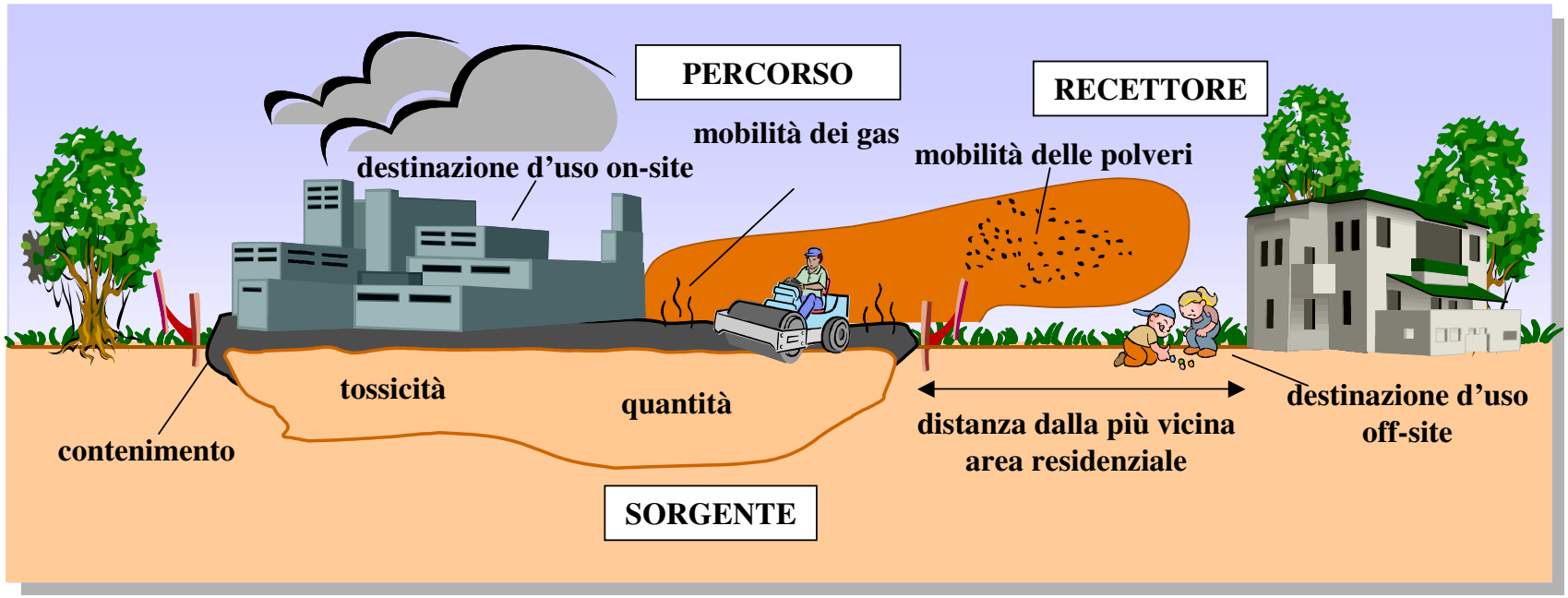

# *Indagini per la caratterizzazione*

***Indagini storiche***

***Indagini sul sito***

***Indagini geognostiche***

***Indagini chimiche***

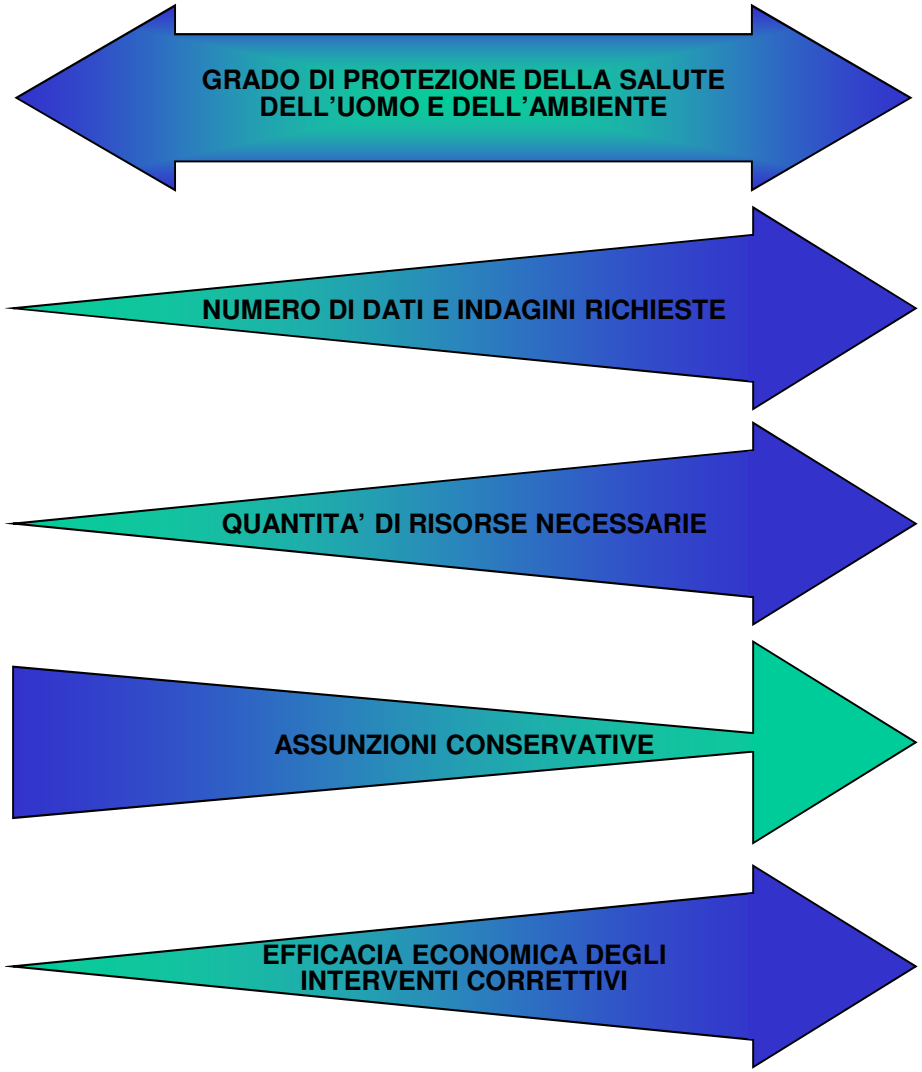

# Modello concettuale per l'analisi di rischio

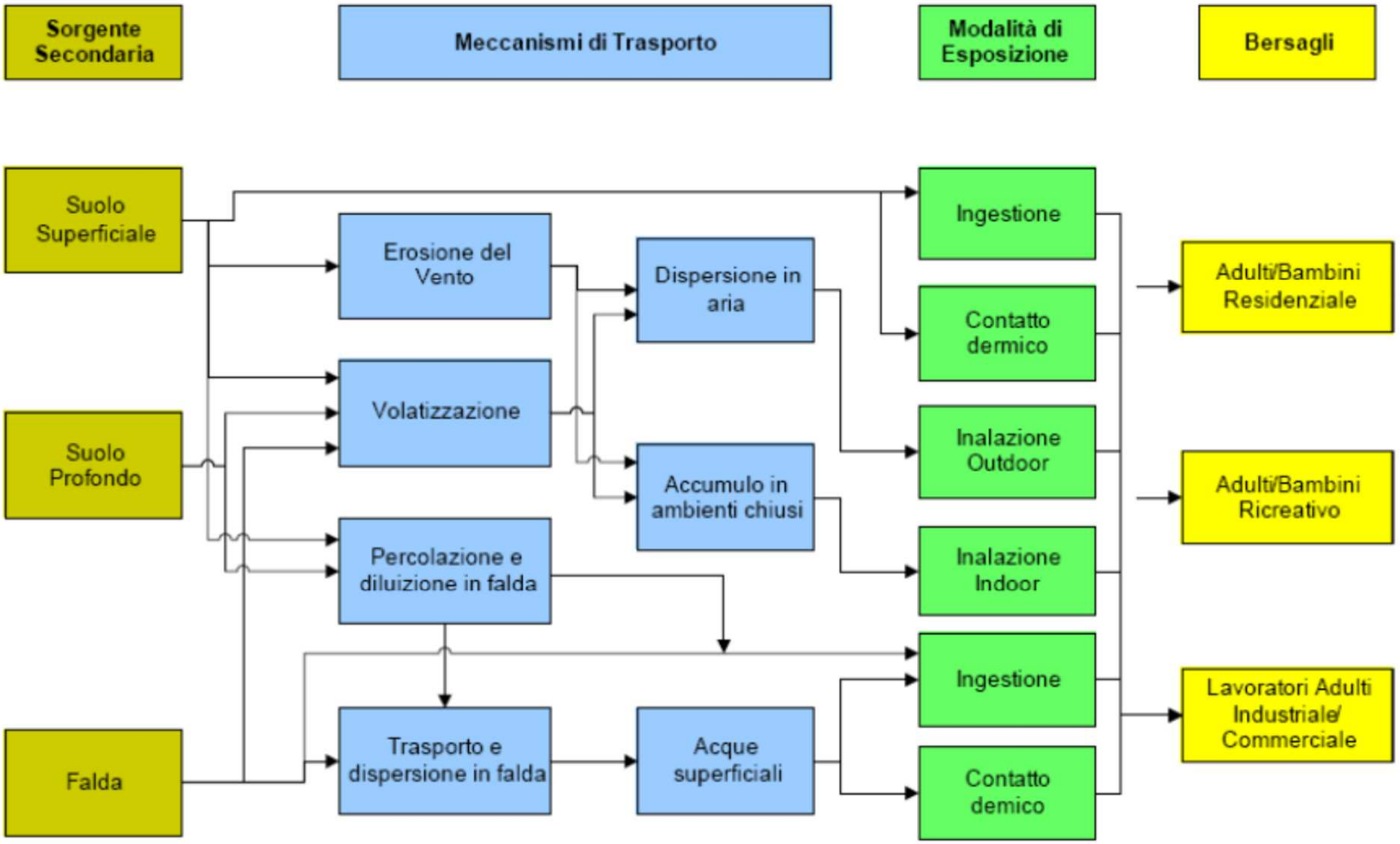

| | mean | var | DevSt. | % CV | SK | Ku | min | 25 % | M | 75 % | max |
|---|---|---|---|---|---|---|---|---|---|---|---|
| SiO2 | 52.94 | 18.21 | 4.27 | 0.08 | - 0.43 | 3.403 | 40.57 | 50.53 | 53.45 | 55.41 | 63.25 |
| TiO2 | 1.15 | 0.01 | 0.11 | 0.09 | 0.04 | 5.79 | 0.78 | 1.08 | 1.15 | 1.21 | 1.57 |
| Al2O3 | 18.74 | 2.37 | 1.54 | 0.08 | - 0.65 | 4.53 | 13.13 | 17.87 | 18.98 | 19.71 | 22.72 |
| FeO | 7.73 | 1.12 | 1.06 | 0.14 | 0.81 | 5.88 | 4.87 | 7.23 | 7.66 | 8.19 | 11.91 |
| MnO | 0.18 | 0.003 | 0.05 | 0.29 | 0.05 | 3.23 | 0.06 | 0.15 | 0.18 | 0.218 | 0.34 |
| MgO | 1.78 | 0.40 | 0.63 | 0.35 | 4.07 | 23.99 | 1.09 | 1.54 | 1.66 | 1.80 | 5.92 |
| CaO | 1.58 | 1.69 | 1.30 | 0.82 | 5.07 | 35.44 | 0.64 | 0.97 | 1.23 | 1.61 | 11.20 |
| Na2O | 0.59 | 0.02 | 0.14 | 0.24 | -0.30 | 3.34 | 0.18 | 0.49 | 0.58 | 0.68 | 0.94 |
| K2O | 1.75 | 0.08 | 0.29 | 0.17 | 0.66 | 3.96 | 1.13 | 1.53 | 1.75 | 1.91 | 2.73 |
| P2O5 | 0.15 | 0.003 | 0.05 | 0.38 | 1.71 | 7.54 | 0.08 | 0.10 | 0.14 | 0.17 | 0.39 |
| L.O.I. | 13.41 | 7.98 | 2.83 | 0.21 | 0.94 | 5.01 | 5.36 | 11.65 | 12.88 | 14.64 | 22.50 |
| Cr | 215.0 | 1852 | 43.03 | 0.20 | 1.57 | 5.58 | 146 | 193 | 204 | 223.7 | 355 |
| Ni | 111.4 | 840 | 28.99 | 0.26 | 1.52 | 7.80 | 48 | 94.25 | 106 | 121.8 | 243 |
| Rb | 134.0 | 625.1 | 25.00 | 0.19 | -0.23 | 3.42 | 71 | 122.5 | 138 | 148 | 202 |
| Nb | 18.23 | 10.22 | 3.20 | 0.18 | -1.41 | 11.68 | 1 | 17 | 18 | 20 | 28 |
| Sr | 94.08 | 221.6 | 14.89 | 0.16 | 3.41 | 27.08 | 62 | 87 | 94 | 100.8 | 197 |
| Zr | 309. 2 | 2746 | 52.40 | 0.17 | -0.03 | 3.89 | 148 | 279.3 | 307 | 340.8 | 459 |
| Y | 51.62 | 78.13 | 8.84 | 0.17 | 2.21 | 10.08 | 37 | 47.25 | 50 | 53 | 95 |
| Ba | 419.4 | 3804 | 61.68 | 0.15 | -0.967 | 4.91 | 170 | 380.3 | 428 | 460.8 | 535 |
| La | 64.89 | 73.10 | 8.55 | 0.13 | -3.85 | 6.12 | 30 | 61 | 65 | 69.75 | 90 |
| Ce | 137.4 | 236.2 | 15.37 | 0.12 | -0.60 | 6.75 | 76 | 131 | 137 | 144 | 183 |
| Nd | 57.85 | 50.58 | 7.12 | 0.12 | -1.16 | 6.83 | 28 | 55 | 58 | 62 | 73 |
| | | | | | | | | | | | |

# Istogrammi

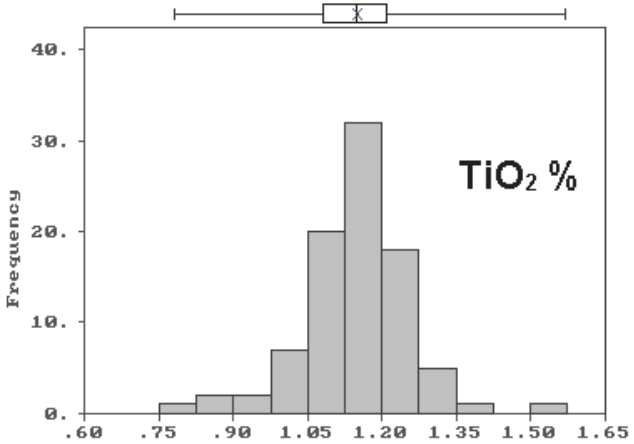
TiO2 %
Frequency
40.
30.
20.
10.
0.
.60
.75
.90
1.05
1.20
1.35
1.50
1.65

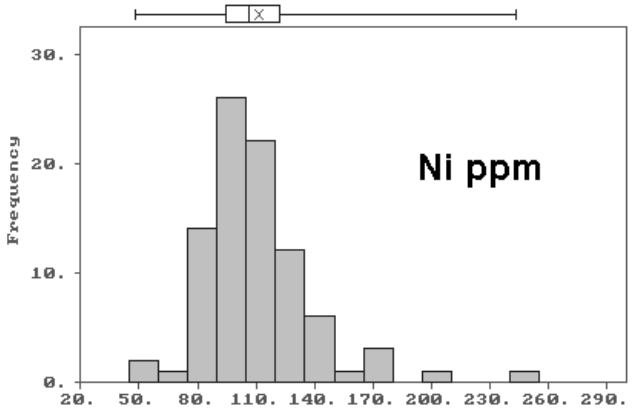
Ni ppm
Frequency
30.
20.
10.
0.
20.
50.
80.
110.
140.
170.
200.
230.
260.
290.

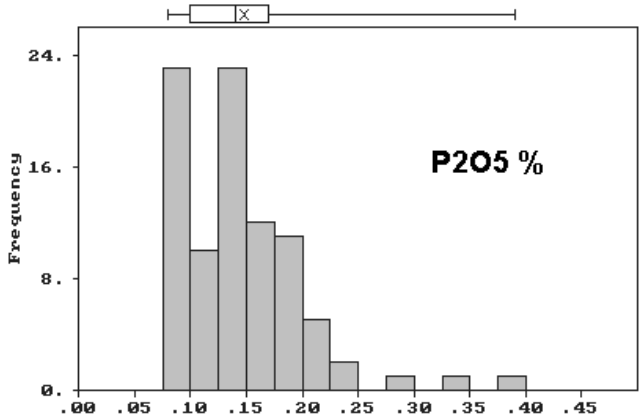
P2O5 %
Frequency
24.
16.
8.
0.
.00
.05
.10
.15
.20
.25
.30
.35
.40
.45

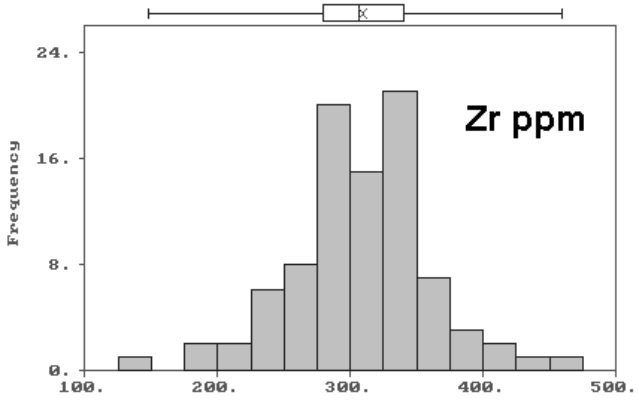
Zr ppm
Frequency
24.
16.
8.
0.
100.
200.
300.
400.
500.

# Curve cumulative

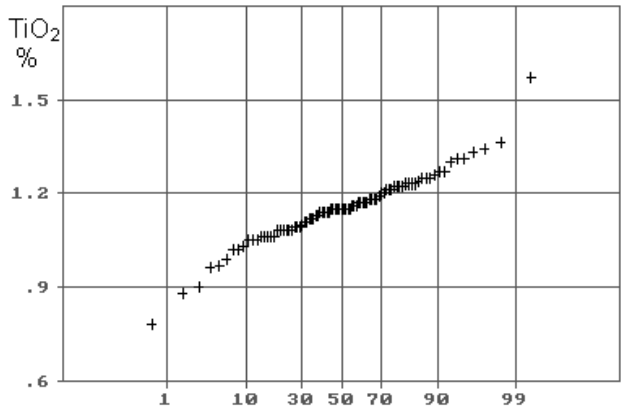


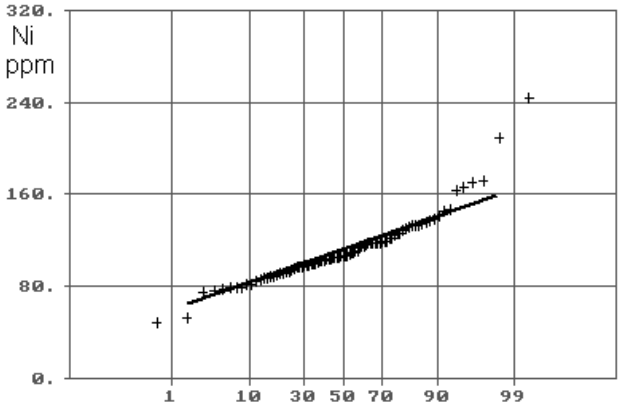


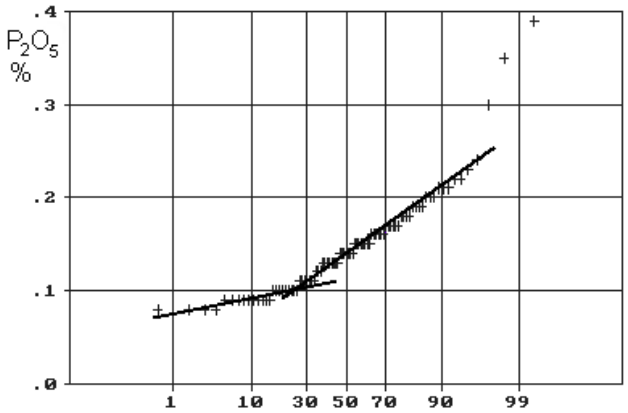


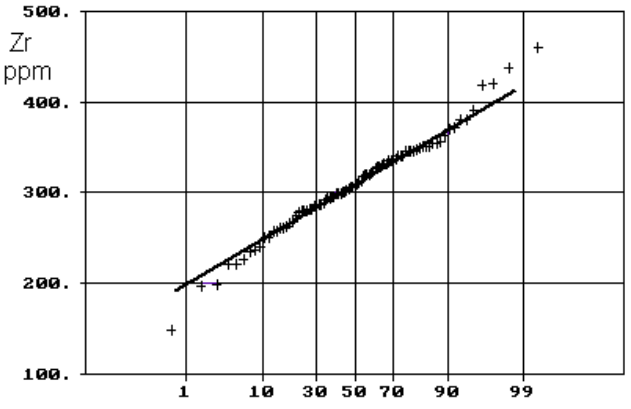

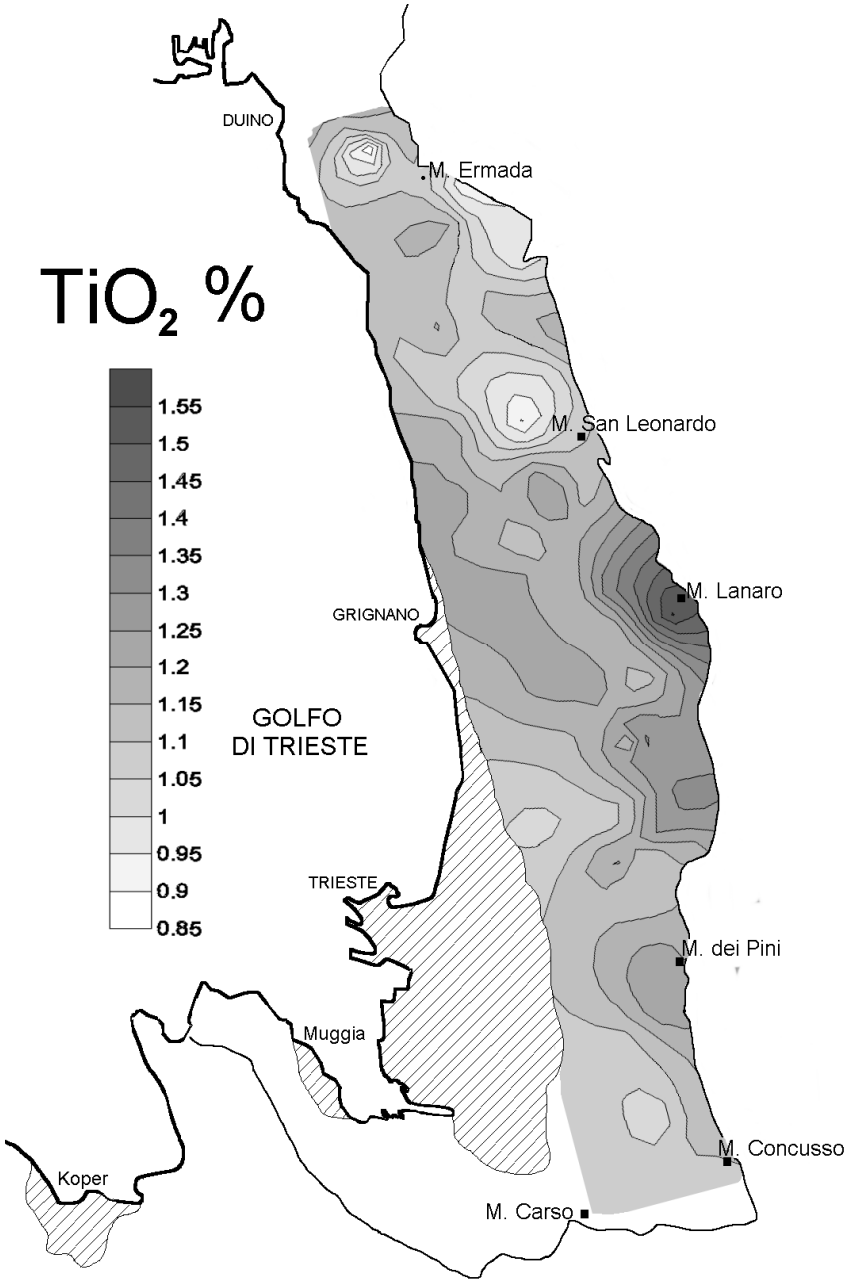
$TiO_2$ %
1.55
1.5
1.45
1.4
1.35
1.3
1.25
1.2
1.15
1.1
1.05
1
0.95
0.9
0.85
DUINO
M. Ermada
M. San Leonardo
M. Lanaro
GRIGNANO
GOLFO
DI TRIESTE
TRIESTE
M. dei Pini
Muggia
M. Concusso
Koper
M. Carso

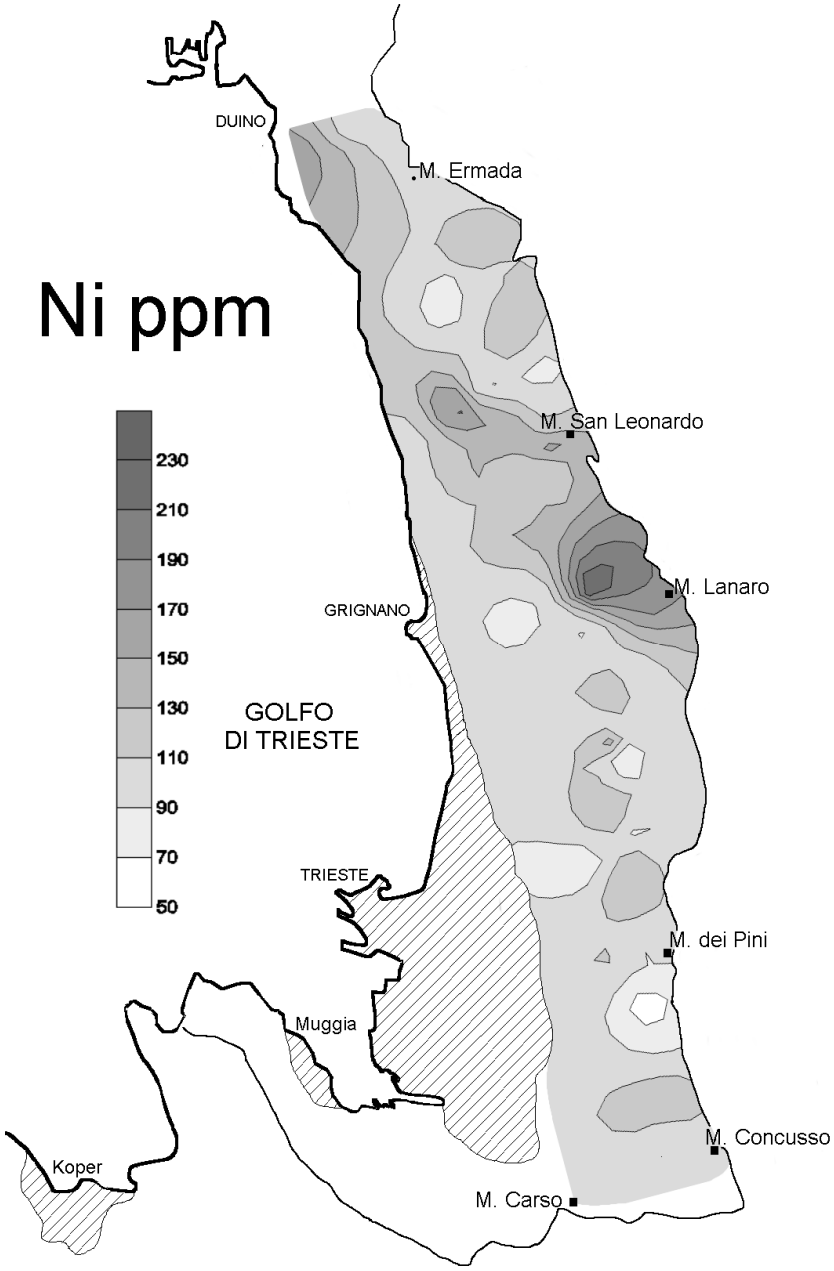
Ni ppm
230
210
190
170
150
130
110
90
70
50
DUINO
M. Ermada
M. San Leonardo
M. Lanaro
GRIGNANO
GOLFO
DI TRIESTE
TRIESTE
M. dei Pini
Muggia
M. Concusso
Koper
M. Carso

# ANALISI DEI CAMPIONI

# Scelta delle tecniche analitiche

*Tabella 10.1* – Tecniche analitiche per la determinazione di metalli potenzialmente tossici in campioni inorganici utilizzati in studi ambientali (compilata sulla base dei dati prodotti da laboratori commerciali, pubblicati nel 2000). I limiti di rilevabilità strumentale sono espressi in ppm, salvo quando diversamente specificato.

| Elemento | Tecniche analitiche | | Limiti di rilevabilità strumentale | | Stato del campione |
|---|---|---|---|---|---|
| | Lab A | Lab B | Lab A | Lab B | |
| As | INAA | | 0,5 | | Solido |
| | AAH | | | 0,1 | Idrato |
| Be | ICP | | 2 | 0,5 | Soluzione |
| Cd | ICP | | 0,5 | | Soluzione |
| | | AA | | 0,2 | |
| Co | INAA | | 1 | | Solido |
| | | ICP | | 1 | Soluzione |
| Cr | INAA | | 5 | | Solido |
| | | XRF | 5 | | Solido |
| Cu | ICP | | 1 | 1 | Soluzione |
| Fe | INAA | | 0,01% | | Solido |
| | | ICP | | 50 | Soluzione |
| Hg | CV-AA | | 5 ppb | 5 ppb | Vapori freddi |
| Mn | ICP | | 1 | 2 | Soluzione |
| Mo | ICP | | 2 | 1 | Soluzione |
| Ni | ICP | | 1 | 1 | Soluzione |
| Pb | ICP | | 5 | 2 | Soluzione |
| Sb | INAA | | 0,1 | | Solido |
| | | AAH | | 0,1 | Idrato |
| Sc | INAA | | 0,1 | | Solido |
| | | ICP | | 0,5 | Soluzione |
| Se | INAA | | 3 | | Solido |
| | | AAH | | 0,1 | Idrato |
| Ti | ICP | | 0,01% | | Soluzione |
| | | XRF | | 5 | Solido |
| V | INAA | | 2 | | Solido |
| | | ICP | | 2 | Soluzione |
| Zn | ICP | | 1 | 1 | Soluzione |

INAA – Analisi per Attivazione Neutronica; AAH – Assorbimento Atomico con Generazione di Idrati; ICP – Plasma Accoppiato Induttivamente, Spettrometria Atomica di Emissione (ICP-AES) = Spettrometria Ottica di Emissione (ICP-OES); AA – Assorbimento Atomico; CV-AA – Assorbimento Atomico con Vapori Freddi; XRF – Fluorescenza a Raggi X.

INAA, ICP-OES, ICP-MS, XRF: possono effettuare analisi multielementali e quindi possono essere determinati contemporaneamente sia gli elementi maggiori costituenti le rocce che i principali elementi metallici di rilevanza neo progetti di geochimica ambientale. ICP-MS rispetto a ICP-OES ha il vantaggio di effettuare analisi con limiti di rilevabilità molto più bassi.

*Tabella 10.2* – Limiti di rilevabilità strumentale di metalli potenzialmente tossici determinati in campioni di vegetazione (in ppm) da un laboratorio selezionato (Lab A). Le analisi di vegetazione del Lab B sono state effettuate solo con INAA. I valori delle acque naturali (in ppb) sono state analizzate con ICP-MS (compilata sulla base dei dati prodotti da laboratori commerciali, pubblicati nel 2000).

| | | **Limiti di rilevabilità strumentale** | | | |
|---|---|---|---|---|---|
| **Elemento** | **Tecnica selezionata** | **Vegetazione** | | **Acque naturali (dolci)*** | |
| | Lab A | Lab A | Lab B | Lab A | Lab B |
| As | INAA | 1 – 0,01 | 0,01 | 0,03 | 0,1 |
| Be | ICP-MS | 0,01 | ND | 0,1 | 0,1 |
| Cd | ICP-OES | 0,1 | 0,5 | 0,01 | 0,01 |
| Co | INAA | 0,1 | 0,3 | 0,005 | 0,1 |
| Cr | INAA | 0,3 | 0,3 | 0,5 | 0,1 |
| Cu | ICP-OES | 0,5 | ND | 0,2 | 0,1 |
| Fe | INAA | 50 | 0,005% | 5 | ND |
| Hg | CV-FIMS | 0,005 | 50 ppb | 0,006 | 0,2 |
| Mn | INAA | 0,01 | ND | 0,1 | 0,1 |
| Mo | INAA | 0,05 | 0,05 | 0,1 | 1 |
| Ni | ICP-MS | 1 | 5 | 0,3 | 0,1 |
| Pb | ICP-MS | 1 | ND | 0,1 | 0,01 |
| Sb | INAA | 0,005 | ND | 0,01 | 0,1 |
| Sc | INAA | 0,01 | 0,2 | 1 | 0,1 |
| Se | INAA | 0,1 | 0,5 | 0,2 | 0,1 |
| Ti | ICP-OES | 2 | ND | 0,1 | ND |
| V | ICP-MS | 0,1 | ND | 0,05 | 0,1 |
| Zn | ICP-MS | 1 | 2 | 0,5 | 0,1 |

ND – non determinato. * I limiti di rilevabilità per le acque marine e le salamoie naturali sono di un ordine di grandezza più grandi. INAA – Analisi per Attivazione Neutronica; ICP-MS – Plasma Accoppiato Induttivamente – Spettrometria di Massa; ICP-OES – Plasma Accoppiato Induttivamente – Spettrometria Ottica di Emissione; CV-FIMS – Flusso di Iniezione (Sistema Mercurio) con Vapori Freddi.

*Tabella 10.3* – Superficie specifica di minerali e suoli adsorbenti, che tendono a far diminuire la solubilità dei metalli (Bourg, 1995)

| **Minerali e suoli** | **Superficie specifica ($m^2$/gm)** |
|---|---|
| Smectite (aka montmorillonite) | 700-800 |
| Illite | 65-100 |
| Kaolinite | 7-30 |
| Ossidi di Mn | 30-300 |
| Ossidi di Fe | 40-80 |
| Argille e terra argillosa | 20-270 |
| Terra argillosa siltosa | 20-200 |
| Rendzina | 15-170 |
| Terra argillosa sabbiosa e sabbia argillosa | 10-70 |
| Sabbia calcarea | 0,5-5 |

*Tabella 10.4* – Mobilità di metalli potenzialmente tossici in ambienti supergenici (esempio, suoli) in diverse condizioni di pH e Eh (da Siegel, 1992).

| **Mobilità relativa** | **Condizioni ossidanti pH 5-8** | **Condizioni ossidanti pH < 4** | **Condizioni riducenti** |
|---|---|---|---|
| Molto mobili | Mo (Se) | | |
| Moderatamente mobili | Zn, V, As (Hg, Sb) | Zn, Cd, Hg, Cu, Co, Ni, V, As, Mn | Mn |
| Leggermente mobili | Mn, Pb, Cu, Ni, Co, (Cd) | | Fe |
| Immobili | Fe, Sc, Ti, Sn (Cr) | Fe, Sc, Ti, Sn, As, Mo, Se | Fe, Ti, Sn, Cu, Pb, Zn, Cd, Hg, Ni, Co, As, Sb, V, Se, Mo, Cr |

Environ Earth Sci (2011) 62:481–491
DOI 10.1007/s12665-010-0541-3

ORIGINAL ARTICLE

# Natural arsenic contamination in waters from the Pesariis village, NE Italy

R. Petrini · F. Slejko · A. Lutman · S. Pison · G. Franceschini · L. Zini · F. Italiano · A. Galic

Arsenic (As) is a widespread element, which usually occurs at trace levels in rocks, soils, and natural waters (Merian 1991; Taylor and McLennan 1995). Despite the fact that As is a bioavailable micronutrient element and essential in a correct diet for humans, the ingestion of excess amounts of As and its bioaccumulation in the human body has a strong harmful impact on health (e.g. Tseng 1977; Morales et al. 2000; Duker et al. 2005; Hopenhayn 2006). The maximum admissible concentration of As in drinking waters has been fixed by the World Health Organization (WHO) at 10 µg/L (WHO 2001). In addition, the US Environmental Protection Agency has placed the thresholds for acute and chronic As toxicity in aquatic ecosystems at 360 and 190 µg/L, respectively, for a water hardness (expressed as $CaCO_3$) of 100 mg/L.

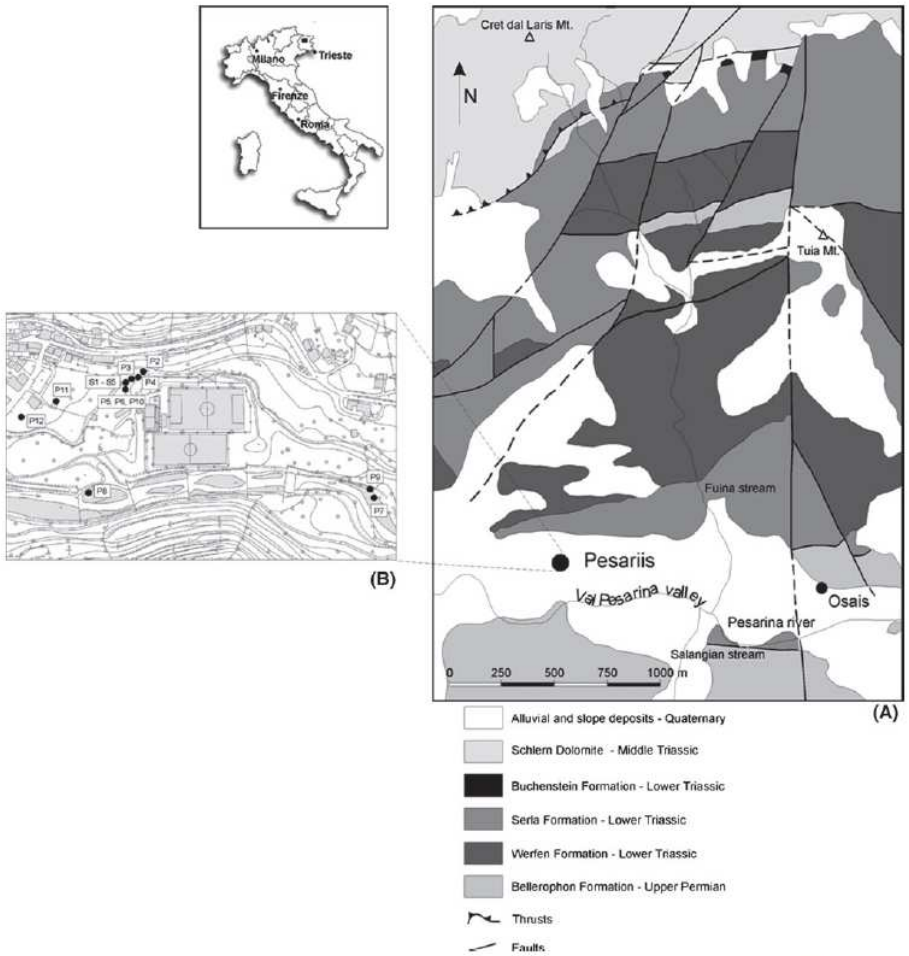


**Fig. 1** a Geological sketch map of the studied area of Val Pesarina, including the village of Pesariis (after Venturini 2002, modified). b Locations of the sampling site in the village of Pesariis

**Table 1** Physico-chemical parameters, major ions and selected trace element data for the studied waters

| Sample | Date of sampling | *T* (°C) | Eh (V) | pH | EC (µS/cm) | Mg (mg/L) | K (mg/L) | Na (mg/L) | Ca (mg/L) | F (mg/L) | $SO_4$ (mg/L) | Cl (mg/L) | $HCO_3$ (mg/L) | Mn (µg/L) | Fe (µg/L) | As (µg/L) |
|---|---|---|---|---|---|---|---|---|---|---|---|---|---|---|---|---|
| Ca–Mg–$SO_4$ type | | | | | | | | | | | | | | | | |
| S1 | 9/13/2006 | 13.7 | 0.17 | 7.4 | 2,409 | 127.1 | 2.0 | 5 | 523.8 | 1.7 | 1,601 | 2 | 201 | nd | 457 | 574 |
| S2 | 10/16/2006 | 13.0 | 0.15 | 7.3 | 2,373 | 123.1 | 1.8 | 6 | 521.2 | 1.7 | 1,596 | 2 | 180 | nd | 439 | 564 |
| S3 | 12/12/2006 | 11.6 | 0.11 | 7.4 | 2,502 | 112.7 | 7.0 | 7 | 489.6 | 1.5 | 1,498 | 5 | 177 | 7 | 582 | 655 |
| S4 | 4/21/2007 | 12.8 | 0.12 | 7.5 | 2,409 | 126.8 | 0.4 | 6 | 508.2 | 1.7 | 1,633 | 2 | 152 | 11 | 884 | 785 |
| S5 | 6/10/2007 | 13.0 | 0.07 | 7.5 | 2,053 | 119.5 | 2.3 | 8 | 502.0 | 15.2 | 1,490 | 13 | 171 | 7 | 804 | 749 |
| P2 | 2/14/2008 | 8.2 | 0.35 | 7.9 | 1,561 | 85.8 | 1.2 | 6 | 309.0 | 1.2 | 935 | 5 | 238 | 3 | <1 | 304 |
| P3 | 2/14/2008 | 12.2 | 0.16 | 7.5 | 2,144 | 120.4 | 0.8 | 5 | 465.4 | 1.4 | 1,493 | 1 | 140 | 8 | 686 | 984 |
| P4 | 2/14/2008 | 10.4 | 0.12 | 7.3 | 2,028 | 103.4 | 0.8 | 5 | 448.3 | 1.3 | 1,344 | 2 | 85 | 13 | 1088 | 992 |
| P5 | 2/14/2008 | 12.3 | 0.13 | 7.3 | 2,216 | 129.9 | 0.8 | 5 | 471.9 | 1.4 | 1,591 | 1 | 85 | 10 | 917 | 633 |
| P6 | 2/14/2008 | 12.6 | 0.15 | 7.7 | 2,117 | 113.6 | 0.9 | 5 | 452.9 | 1.4 | 1,450 | 1 | 100 | 13 | 450 | 546 |
| P9 | 2/14/2008 | 8.7 | 0.20 | 7.9 | 855 | 43.4 | 2.6 | 6 | 147.5 | 0.4 | 349 | 6 | 177 | 1 | 73 | 114 |
| P10 | 2/14/2008 | 11.8 | 0.14 | 7.4 | 2,166 | 123.4 | 0.8 | 5 | 464.2 | 1.4 | 1497 | 1 | 134 | 9 | 860 | 716 |
| Ca–$HCO_3$–$SO_4$ type | | | | | | | | | | | | | | | | |
| P7 | 2/14/2008 | 4.3 | 0.34 | 8.2 | 537 | 25.3 | 0.6 | 2 | 88.6 | 0.1 | 178 | 2 | 122 | nd | <1 | 8 |
| P8 | 2/14/2008 | 8.6 | 0.40 | 8.2 | 510 | 23.6 | 0.5 | 2 | 83.5 | 0.1 | 163 | 2 | 73 | nd | <1 | 1 |
| P11 | 6/19/2008 | 8.5 | 0.22 | 7.7 | 473 | 23.3 | 1.0 | 4 | 72.8 | 0.2 | 112 | 6 | 213 | <1 | <1 | 4 |
| P12 | 6/19/2008 | 8.7 | 0.20 | 7.5 | 642 | 30.8 | 1.5 | 7 | 104.3 | 0.4 | 230 | 9 | 207 | <1 | <1 | 24 |

| | Li (µg/L) | B (µg/L) | Al (µg/L) | Co (µg/L) | Ni (µg/L) | Cu (µg/L) | Zn (µg/L) | Rb (µg/L) | Mo (µg/L) | Cs (µg/L) | Ba (µg/L) | Pb (µg/L) | U (µg/L) | Si (µg/L) |
|---|---|---|---|---|---|---|---|---|---|---|---|---|---|---|
| S4 | 11.27 | 28.22 | 0.35 | 1.29 | 0.56 | 0.79 | 4.09 | 0.94 | 0.97 | 0.14 | 9.67 | 0.17 | 0.40 | 6,596 |
| S5 | 10.95 | 42.87 | 2.19 | 0.96 | 0.42 | 0.15 | 4.32 | 0.92 | 1.10 | 0.16 | 9.41 | 0.08 | 0.34 | nd |

*nd* not determined

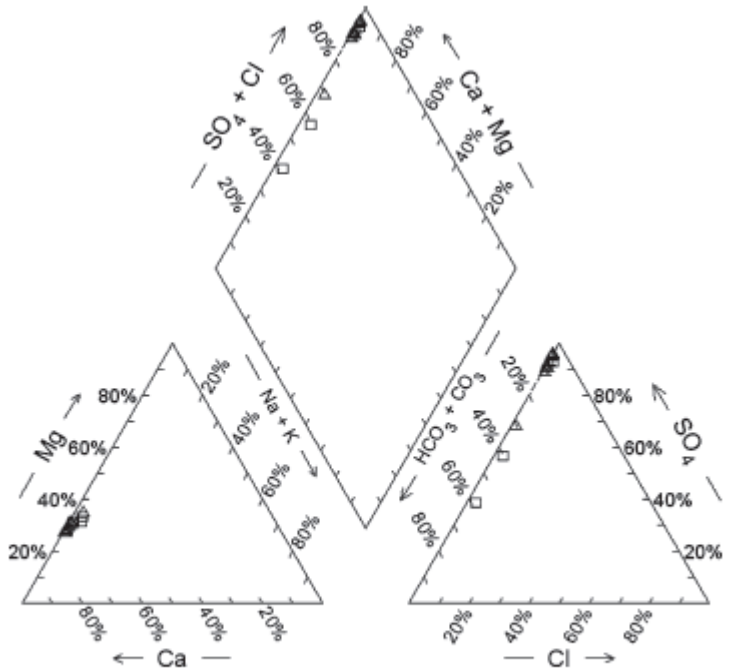


**Fig. 2** Piper diagram. Ca–Mg–$SO_4$ (*open triangle*) and Ca–$HCO_3$–$SO_4$ (*open square*) waters are distinguished

The Ca–Mg–$SO_4$-type groundwaters from the Solfar Spring and the nearby drainages are characterized by the highest As (546–992 µg/L) and Fe content (450–1,088 µg/L)

The Ca–$HCO_3$–$SO_4$ groundwaters have As concentration between 4 and 24 µg/L. Water from the Pesarina River seems to be also affected by the admixing of As-rich waters, increasing the As concentration from 1 to 8 µg/L from downstream to the Pesariis village.

Speciation calculations indicate that the $As^{5+}$ species $HAsO_4^{2-}$ and $H_2AsO_4^-$ are the dominant forms of As in both the Ca–Mg–$SO_4$ and Ca–$HCO_3$–$SO_4$ groundwaters at the sampling sites. $HAsO_3F^-$, $AsO_4^{3-}$, $AsO_3F^{2-}$ and $H_3AsO_4$ are also stable in decreasing abundance. The $As^{3+}$oxo-anions arsenite $As(OH)_3$ and $As(OH)_4^-$ are minor species. Speciation also indicates that Ca–Mg–$SO_4$ waters are strongly undersaturated in arsenic sulfide minerals, such as orpiment ($As_2S_3$) and realgar (AsS).

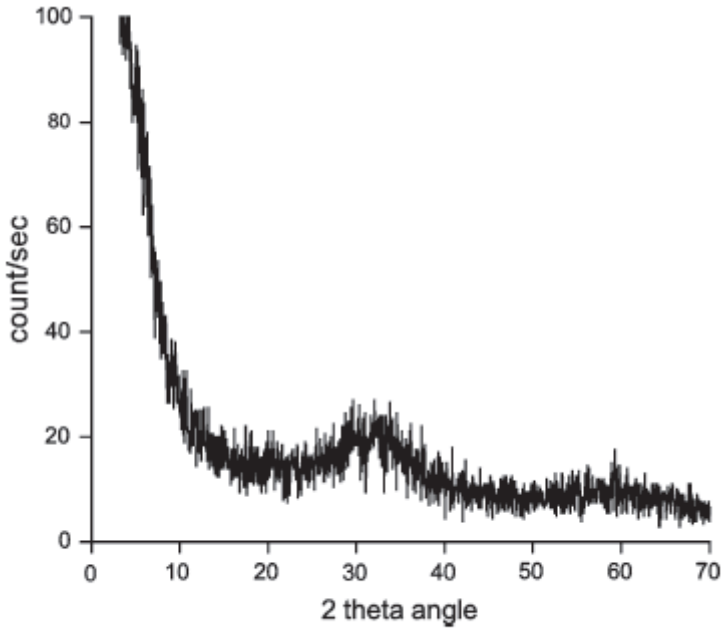


**Fig. 3** XRD diffraction pattern for the iron-rich sediment (sample 1404) at the Solfar Spring outlet

**Table 2** Concentration of selected elements in sediments, marcasite and oxidized marcasite

| Sample | As (mg/kg) | Fe (mg/kg) | Al (mg/kg) | Mn (mg/kg) | Ca (mg/kg) | Mg (mg/kg) |
|---|---|---|---|---|---|---|
| 1404 | 110,000 | 330,000 | 320 | 620 | 57,000 | 3,600 |
| 1405 | 100,000 | 280,000 | 760 | 170 | 80,000 | 3,700 |
| 1406 | 15 | 14,000 | 26,000 | 240 | 290,000 | 38,000 |
| 1407 | 4.1 | 10,000 | 17,000 | 210 | 450,000 | 54,000 |
| Oxidized marcasite | 45 | 640,000 | nd | nd | nd | nd |
| Marcasite | 170 | 270,000 | nd | nd | nd | nd |

*nd* not determined

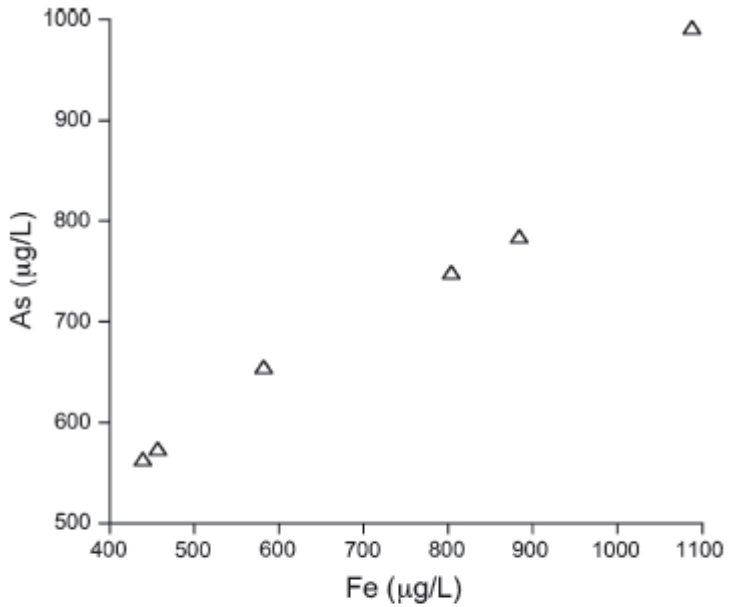


**Fig. 7** Fe versus As correlation diagram for the Ca–Mg–$SO_4$ waters of the Solfar Spring and related drainages. Samples P3 and P5, belonging to different drainages with variable flow rates, are not included in the figure. Ca–Mg–$SO_4$ (*open triangle*) and Ca–$HCO_3$–$SO_4$ (*open square*) waters are distinguished

Ground and surface waters from the village of Pesariis, in the Carnic Alps, are characterized by high As concentrations. The primary source of As is the arsenian marcasite, which forms a sulfide mineral related to the volcanic activity that characterized the area during Lower Triassic. The oxidative weathering of marcasite releases Fe and As to solution during runoff, which is then removed from the solution by adsorption on HFO particles and transported into anoxic environments at depth. The reductive HFO dissolution and As desorption produce polluted subsurface water, which supplies the feeder aquifer of the Ca–Mg–$SO_4$ groundwaters. At the outlet, the extensive formation and settling of amorphous hydrous ferric oxide sediments strongly scavenge As from the aqueous phase.

Water of the As-polluted Ca–Mg–$SO_4$ reservoir mixes at different layers with the shallower aquifers drained by a number of fountains in the village of Pesariis and neighborhoods, and disperses in the aquatic environment through superficial waters.

Estuarine, Coastal and Shelf Science 113 (2012) 20–31

Contents lists available at SciVerse ScienceDirect

Estuarine, Coastal and Shelf Science

journal homepage: www.elsevier.com/locate/ecss


# Mercury in the sediments of the Marano and Grado Lagoon (northern Adriatic Sea): Sources, distribution and speciation

Alessandro Acquavita [a,b], Stefano Covelli [b,*], Andrea Emili [b], Daniela Berto [c], Jadran Faganeli [d], Michele Giani [e], Milena Horvat [f], Neža Koron [d,f], Federico Rampazzo [c]

[a] *Osservatorio Alto Adriatico, Agenzia Regionale per la Protezione dell'Ambiente del Friuli Venezia Giulia (ARPA-FVG), Via Cairoli 14, 33057 Palmanova, Italy*
[b] *Dipartimento di Matematica & Geoscienze, Università di Trieste, Via Weiss 2, 34128 Trieste, Italy*
[c] *ISPRA, Loc. Brondolo, 30015 Chioggia, Venezia, Italy*
[d] *Marine Biological Station, National Institute of Biology, Fornače 41, 6330 Piran, Slovenia*
[e] *Istituto Nazionale di Oceanografia e di Geofisica Sperimentale, Via Piccard 54, 34151 S.Croce, Trieste, Italy*
[f] *Dept. of Environ. Sciences, "Jožef Stefan" Institut, Jamova 39, 1000 Ljubljana, Slovenia*

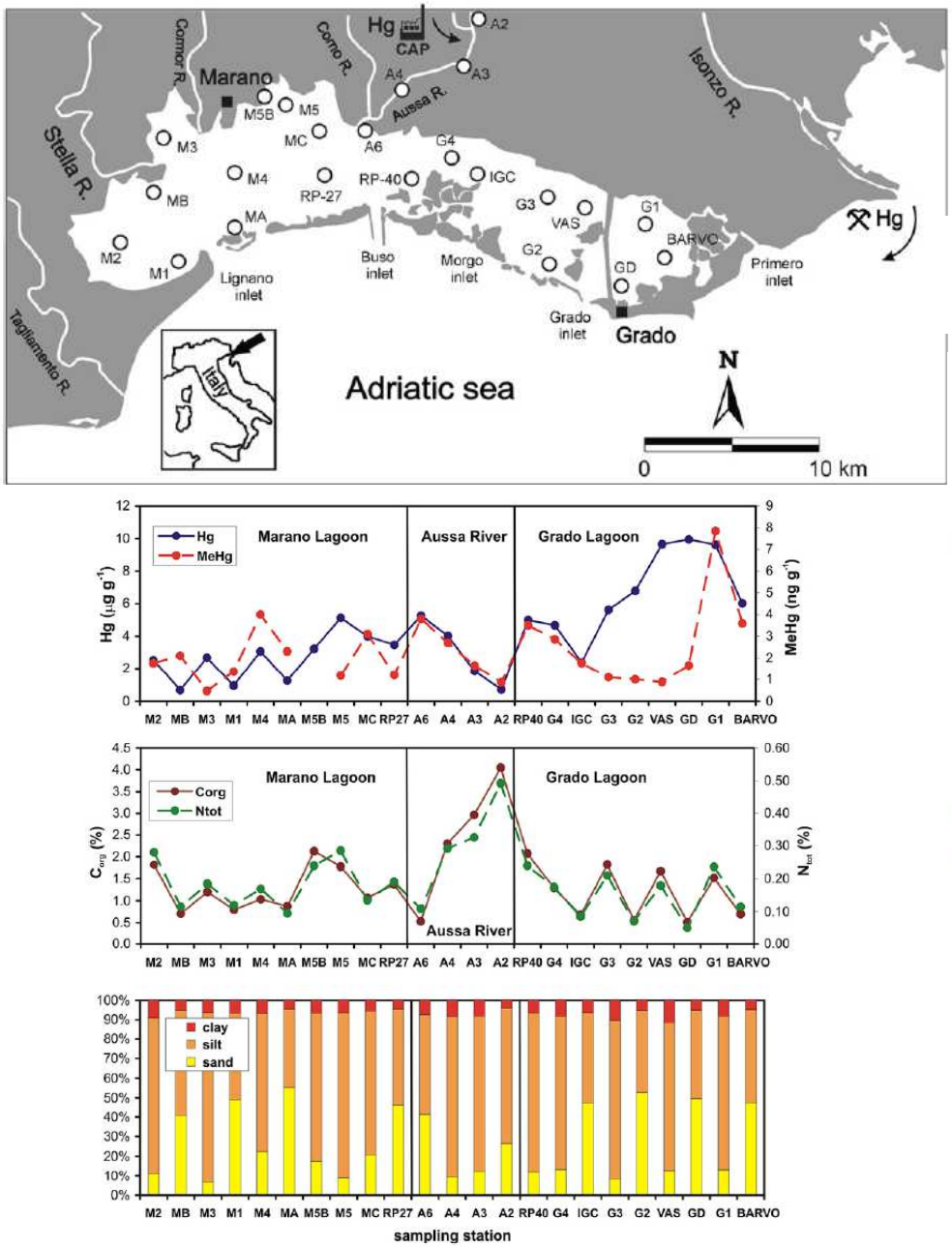


**Fig. 2.** Concentrations of (a) Hg and MeHg; (b) $C_{org}$ and $N_{tot}$; and (c) percentages of the main grain-size fractions (sand, silt, clay) in the sampling sites, which are ordered from west (left) to east (right).

Among the pollutants affecting the Lagoon, mercury (Hg) is the main concern. This element is known to exert neurotoxic and genotoxic effects on humans once transformed into the bioaccumulable organometallic form monomethylmercury (MeHg; Clarkson, 1998; Crespo-López et al., 2007, 2011; Li et al., 2010). The Lagoon is subject to two sources of Hg. Suspended matter originating from the Soča/Isonzo River drainage basin has been responsible for contamination in the Northern Adriatic Sea since the 16th century (Horvat et al., 1999; Covelli et al., 2001). In fact, in over 500 years of mining in Idrija (Northwest Slovenia), 12 million tons of Hg ore have been excavated, of which more than 35,000 t have been lost into the environment during smelting (Kotnik et al., 2005). The Idrija Hg mine finally closed in 1996; however, Hg is still being delivered to the Gulf of Trieste, where concentrations of up to 30 $\mu g\,g^{-1}$ have been reported in sediments (Covelli et al., 2001), and the adjacent Lagoon (Covelli et al., 2007). In addition, Hg was employed as a catalyst in a chlor-alkali plant (CAP) and discharged in an uncontrolled manner from 1949 to 1984 into the Aussa–Corno River system. This system is connected to the central sector of the Lagoon (Piani et al., 2005), where it is estimated that approximately 186 t (with a maximum of 20 kg $day^{-1}$) of Hg have been deposited. Covelli et al. (2009) stated that, although uncontrolled Hg discharge from the CAP has ceased, the artificial channel connecting this industrial area to the Aussa River still acts as an active Hg source. Indeed, studies have revealed high Hg levels in sediments (Brambati, 2001), as well as evidence of bioaccumulation along the trophic chain.

**Table 2**
Ranges of mercury concentration in sediments of northern Adriatic coastal environments as reported in the last 15 years (na = not available).

| Location | THg ($\mu g\,g^{-1}$ d.w.) | MeHg ($ng\,g^{-1}$ d.w.) | Authors | Notes |
|---|---|---|---|---|
| Marano and Grado Lagoon | 1.62–10.6 | na | Brambati, 1997 | Surface sediment (grab and cores). Data refers to the 1992 campaign. |
| | 0.13–6.58 | na | Piani et al., 2005 | Surface sediment (grab). Central sector (Buso basin). |
| | 0.40–0.57 | na | Sfriso et al., 2008 | Marano Lagoon. |
| | 9.5–14.4 | 0.2–17.1 | Covelli et al., 2008 | Top 0–10 cm surface sediment (core). Grado Lagoon. |
| | 0.68–9.95 | 0.47–7.85 | This study | Top 0–1 cm surface sediment (core). Marano and Grado Lagoon. |
| Venice Lagoon | 0.64–3.41 | 0.40–1.56 | Bloom et al., 2004 | Top 0–3 cm surface sediment (core). Northern lagoon. |
| | 0.1–3.4 | na | Berto et al., 2006 | Top 0–3 cm surface sediment (grab). Southern lagoon. |
| | <0.1–2.1 | na | Bernardello et al., 2006 | Top 0–5 cm surface sediment (core). Data refers to the 1998 sampling. |
| | 0.5–4.8 | na | Zonta et al., 2007 | Top 0–10 cm surface sediment (core). Northern Tresse Island samples are excluded. |
| | 0.10–1.22 | na | Sfriso et al., 2008 | Central Venice Lagoon. |
| Pialassa Baiona (Ravenna) | 0.13–250 | 0.13–44.6 | Trombini et al., 2003 | Top 0–5 cm surface sediment (core). |
| | 11–43 | na | Matteucci et al., 2005 | Top 0–3 cm surface sediment (core). Southern ponds (2000–2002). |
| | 0.88–38.0 | na | Fabbri et al., 2006 | Top 0–5 cm surface sediment (core). |
| | 0.37–5.51 | na | Guerra et al., 2009 | Top 0–5 cm surface sediment (box corer). |
| | 14.4–79.0 | 2.1–13.04 | Covelli et al., 2011 | Top 0–7 cm surface sediment (core). Data refers to one sample at Chiaro Magni site. |
| Northern Adriatic Sea | 0.12–1.93 | na | Giani et al., 1994 | Top 0–2 cm surface sediment (core). Ravenna Harbor entrance. |
| | 0.13–0.51 | na | Giani et al., 1994 | Top 0–2 cm surface sediment (core). Offshore Ravenna Harbor entrance. |
| | 0.05–0.23 | na | Fabbri et al., 2001 | Top 0–1 cm surface sediment. Sediment cores collected in front of the Po River delta. |
| Gulf of Trieste | 0.10–23.3 | 0.2–60.1 | Covelli et al., 2001 | Top 0–2 cm surface sediment (core). |
| | <0.4–14.92 | na | Acquavita et al., 2010 | Top 0–5 cm surface sediment (core). |
| | 0.77–4.02 | 0.13–1.07 | Emili et al., 2011 | Top 0–3.5 cm surface sediment (core). Data refer to AA1 and CZ (center of the Gulf). |
| Kaštela Bay (Croatia) | 17.6–74.0 | 6.05–16.4 | Kwokal et al., 2002 | Top 0–1 cm surface sediment (core). |

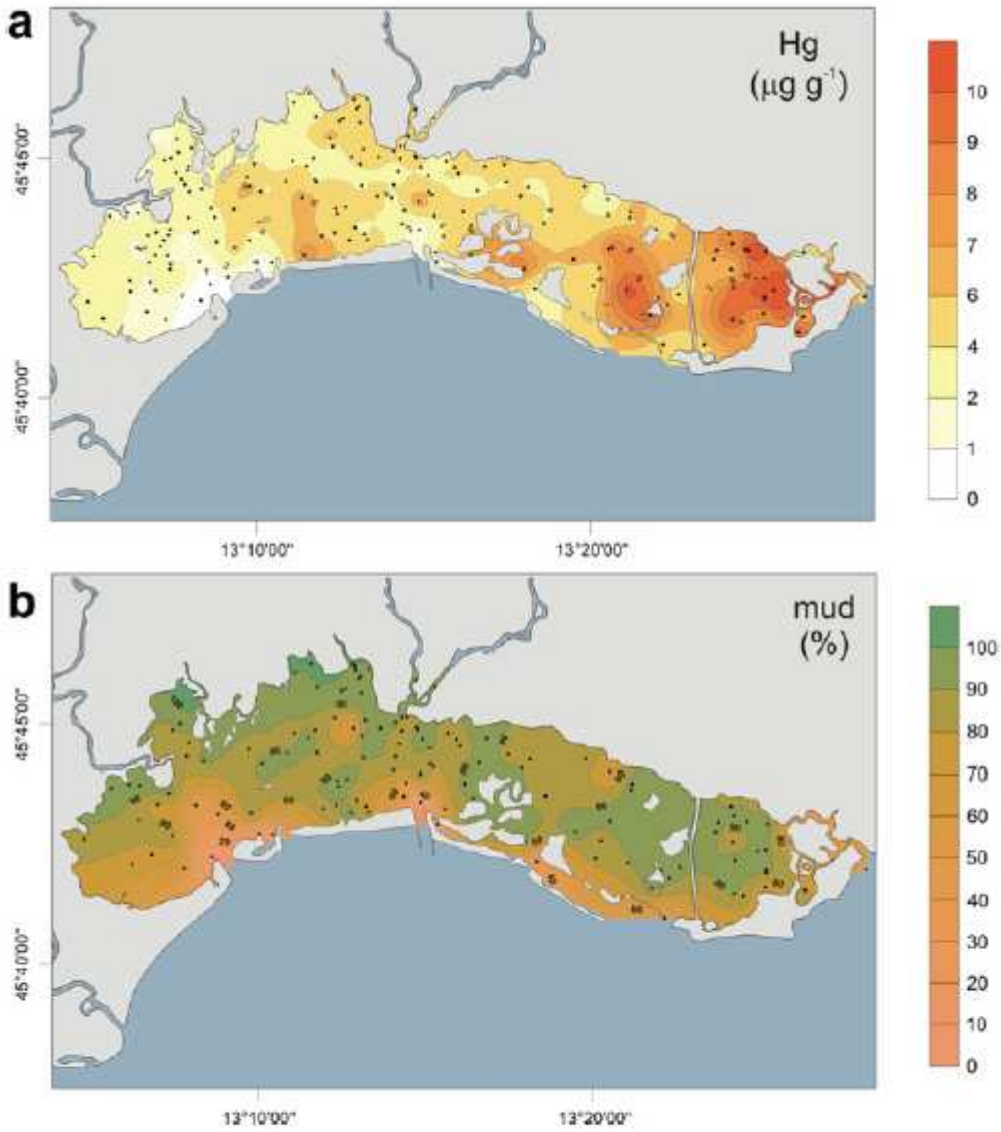


**Fig. 5.** (a) Areal distribution of Hg concentrations in surface sediments of the Lagoon. Data used for this representation were taken from the results of previous studies (RAFVG, 1991; Marocco, 1995; Brambati, 1997; Viso, 2004; Piani et al., 2005). (b) Map of the fine component (<63 μm) distribution in the surface sediments of the Lagoon.

# Miniera di Salafossa


## 2. Study area

The general area of the study is located in the eastern Dolomites belonging to the Alps, within the Veneto region (Northeastern Italy) and along the Piave River (Fig. 1). The region is characterized by an alpine climate with cool summers and cold snowy winters. Spring and autumn are fresh, windy and rainy.

The Salafossa mining area was one of the largest Pb/Zn-containing mineral deposits in Europe. Both metals were mainly present as sulphides: *sphalerite* (ZnS) and *galena* (PbS). The mineral deposit belongs to a unique ore body included in the Ladinian-Carnian Dolomites of the Lower Triassic (Assereto et al., 1977).

Mining activity started around 1550, but it was only around 1960 when the richest veins of the minerals were discovered. From the Salafossa mineral deposits, a little more than 11 million tons of *tout-venant* (raw material), with an average content of 0.9% for Pb and 4.7% for Zn, were extracted. On the whole, 92,000 tons of Pb and 482,000 of Zn were recovered from the mineral deposit (Zas Friz, 1999). The mining activity continued until 1985, the year of its final closure.

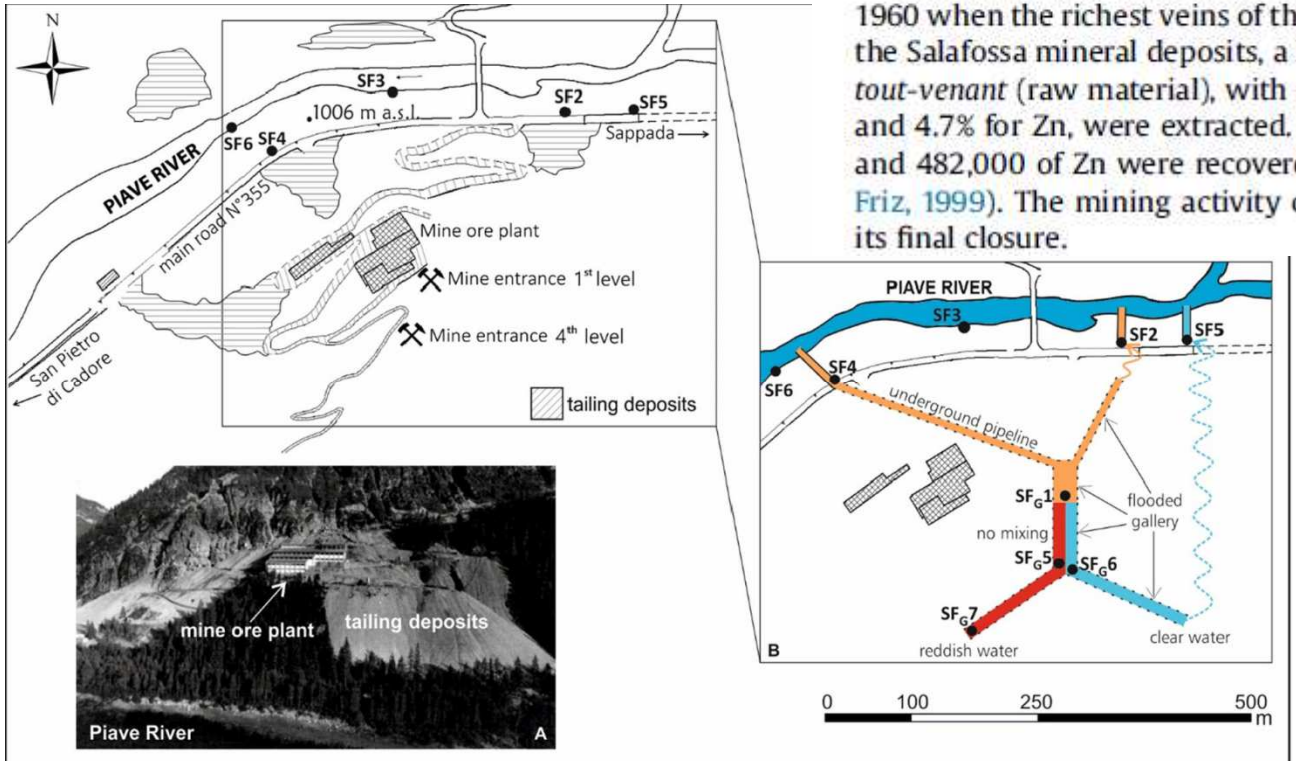

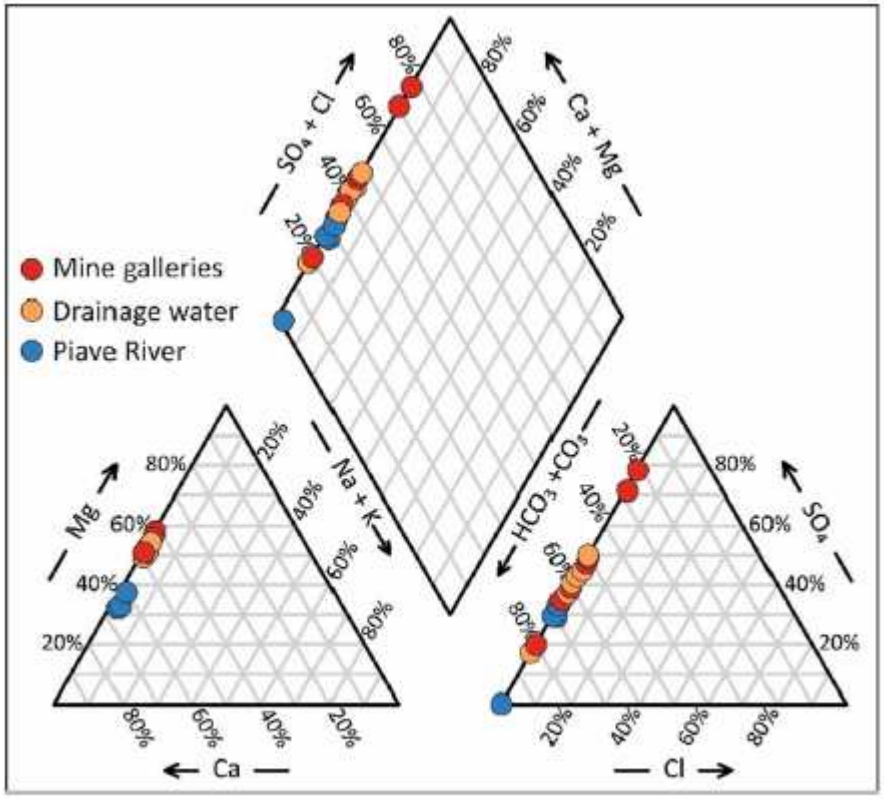


**Fig. 2.** Piper diagram showing the hydrochemical facies of the three types of waters collected from the mine galleries, the drainage outflow and the main river.

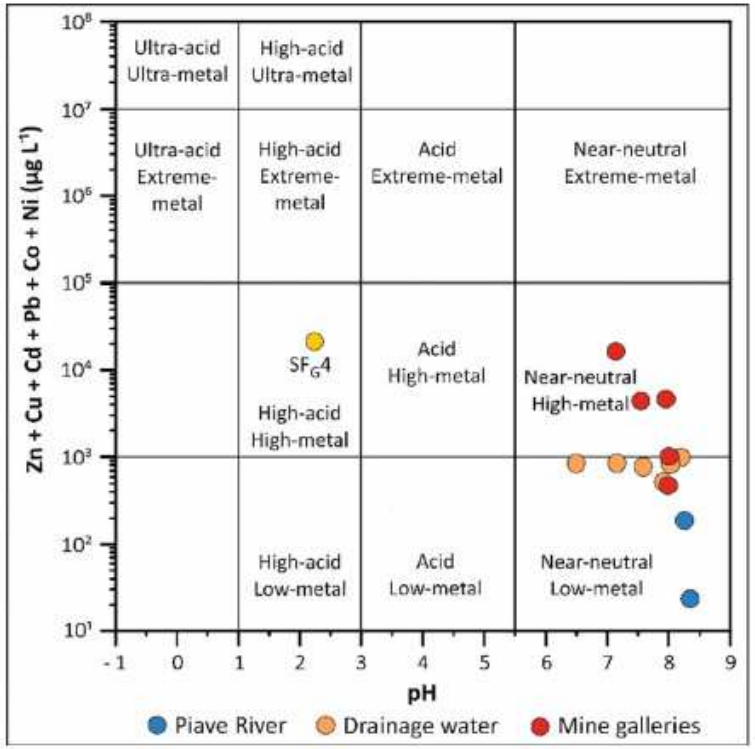


**Fig. 3.** Ficklin diagram of the Salafossa drainage waters showing the sum of dissolved PHEs (Zn, Cu, Cd, Pb, Co, Ni) plotted against pH value.

$$CaCO_{3\,(s)} \rightleftharpoons Ca^{2+} + CO_3^{2-}$$

$$CO_3^{2-} + H_2O \rightleftharpoons HCO_3^- + OH^- \quad (1)$$

$$PbS + 2O_2 \longrightarrow Pb^{2+} + SO_4^{2-} \quad (2)$$

$$ZnS + 2O_2 \longrightarrow Zn^{2+} + SO_4^{2-} \quad (3)$$

$$4FeS_2 + 10H_2O + 15O_2 \rightarrow 4FeO(OH) + 16H^+ + 8SO_4^{2-} \quad (4)$$

$$ZnS + 8Fe^{3+} + 4H_2O \longrightarrow Zn^{2+} + 8Fe^{2+} + SO_4^{2-} + 8H^+ \quad (5)$$

$$ZnS + 2H^+ \rightarrow Zn^{2+} + H_2S \quad (6)$$

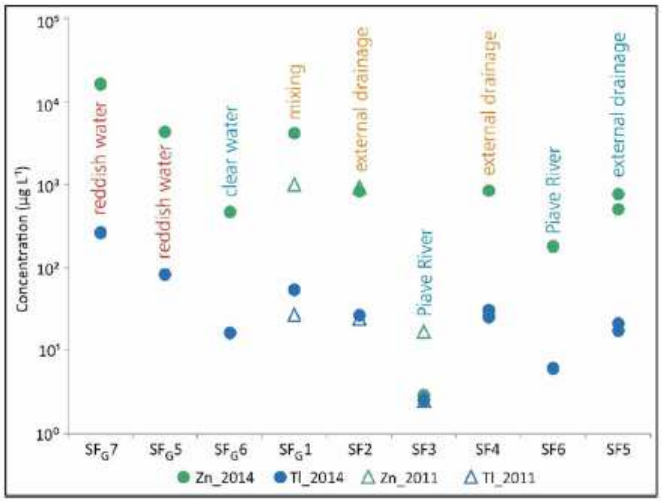


**Fig. 4.** Effect of dilution process observed for Zn and Tl in the drainage waters flowing from the inner part of the mine towards the Piave River.

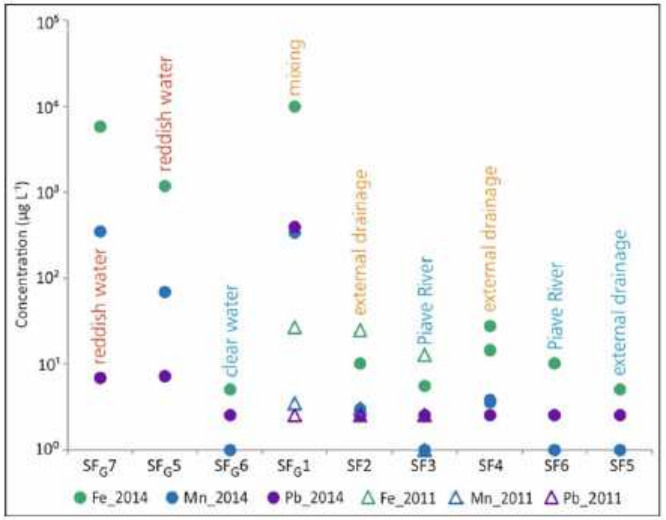


**Fig. 5.** Effect of dilution process observed for Pb, Fe and Mn in the drainage waters flowing from the inner part of the mine towards the Piave River.

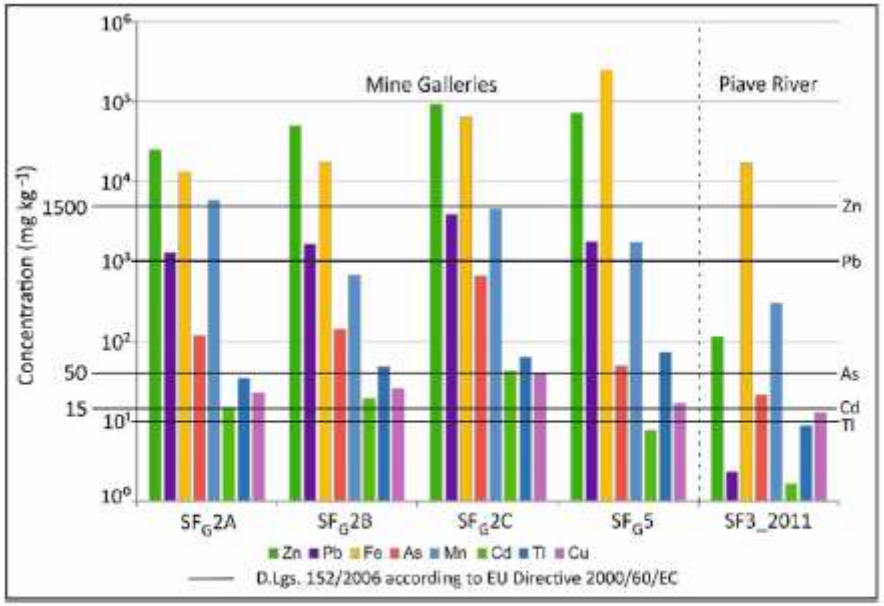


**Fig. 6.** Comparison of PHEs concentrations observed in fine sediment samples collected at the bottom of the mine galleries and at the banks of the Piave River.

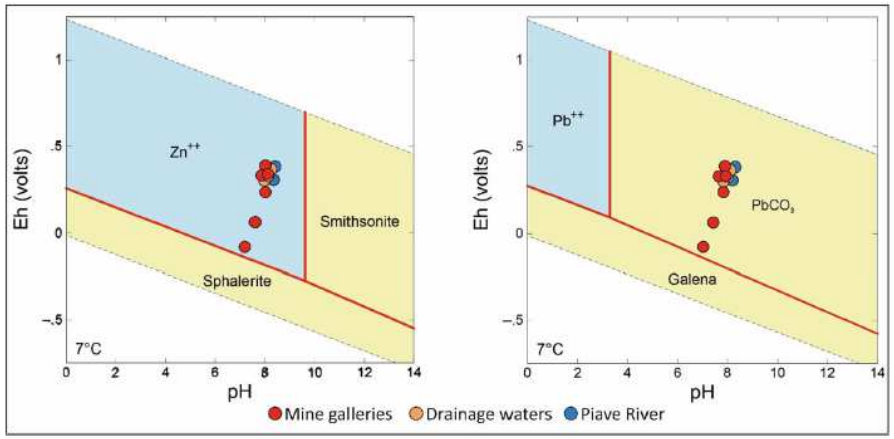


**Fig. 7.** Eh-pH diagram showing the predominant species in water for Zn and Pb according to the average composition and temperature measured at the sampling points.

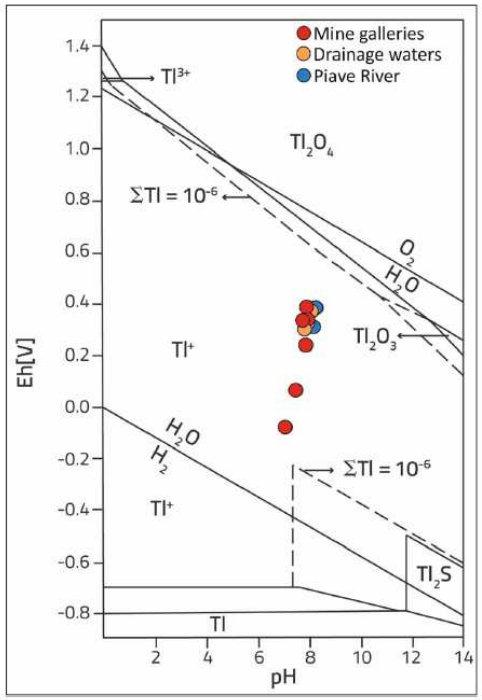


**Fig. 8.** Eh-pH diagram showing the predominant species for Tl in water (from Vink, 1993).

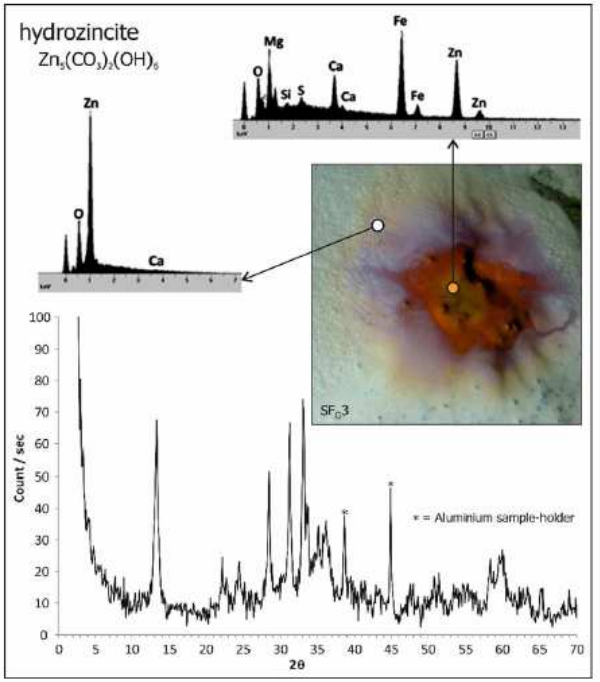


**Fig. 10.** Chemical and mineralogical composition of the mineral concretions sampled in the gallery of the upper level.

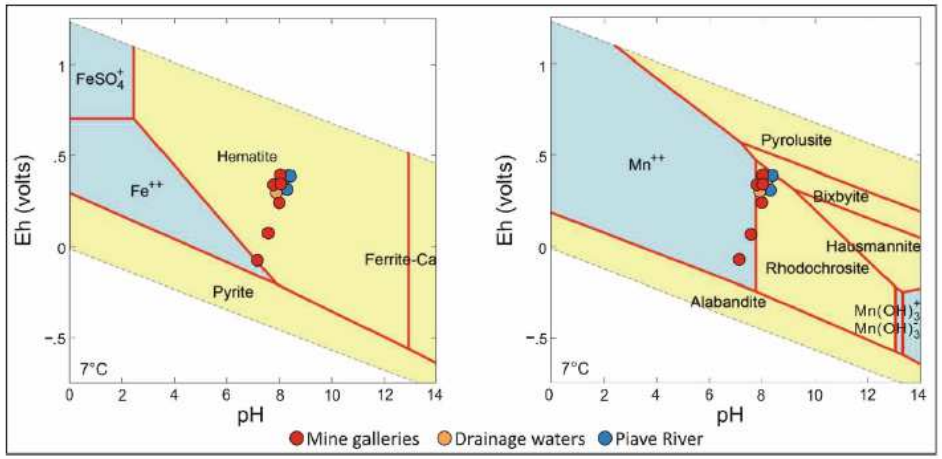


**Fig. 9.** Eh-pH diagram showing the predominant species in water for Fe and Mn according to the average composition and temperature measured at the sampling points.

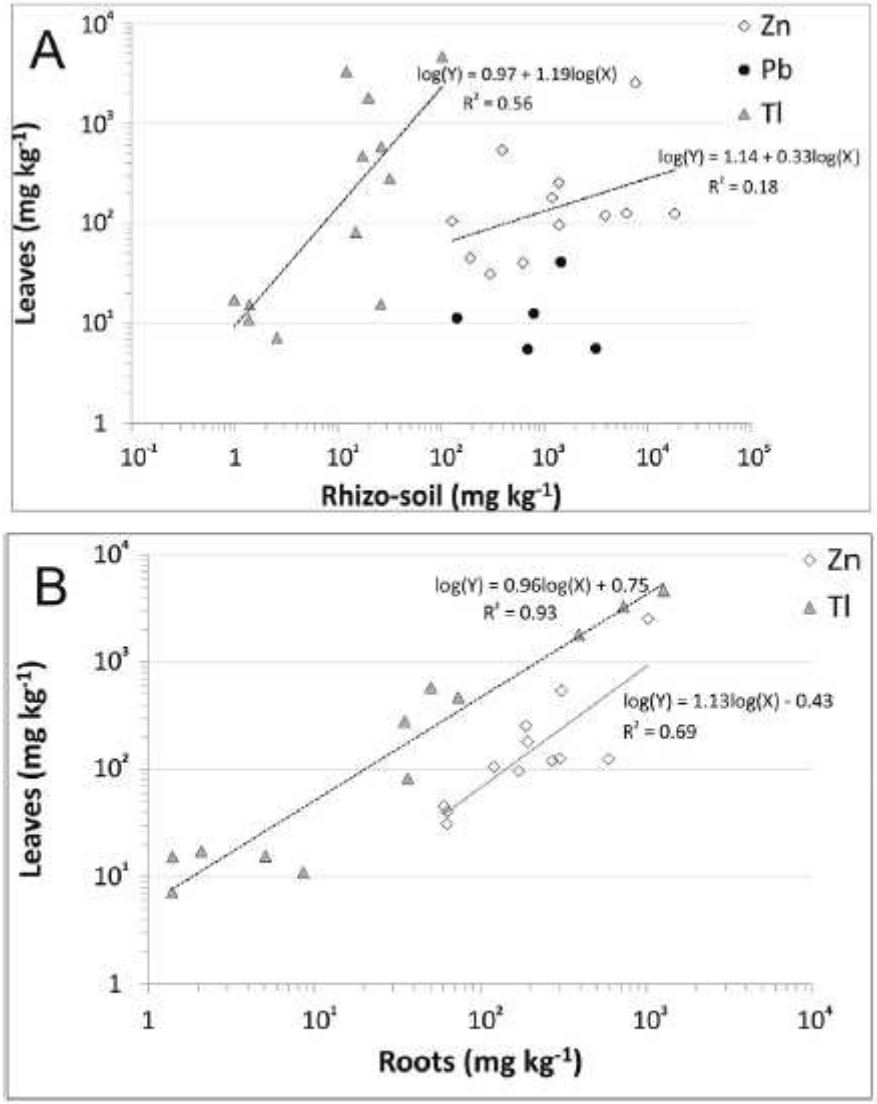


**Fig. 4.** A) Relationships between total metal concentrations of Zn, Pb and Tl measured in the rhizo-soil and in the leaves of *B. laevigata* samples. B) Relationships between metal concentrations of Zn and Tl in roots and leaves of *B. laevigata* samples.

To assess the uptake and translocation processes of the trace metals resulting in their bioaccumulation, two different indices were calculated: the *enrichment factor in roots* (EFr) and the *translocation factor* (TF) (Zhao et al., 2003; Petranich, 2010-2011; Fellet et al., 2012) (Table 4).

The EFr, as the ratio between metal concentration in below-ground biomass and total concentration of the same metal in the respective rhizo-soil, allows for the evaluation of the metal uptake by the root system (2).

$$EF_r = [Me]_{roots}/[Me]_{rhizo-soil} \quad (2)$$

On the other hand, the metal translocation processes from roots to the upper tissues can be determined by the TF, as the ratio between metal concentration in the leaves and in the corresponding roots (3).

$$TF = [Me]_{leaves}/[Me]_{roots} \quad (3)$$

**Table 4**
EFr and TF values (n.d.: non determined).

| Enrichment factor in roots – $EF_r$ | | | | | | Translocation factor – TF | | | | |
|---|---|---|---|---|---|---|---|---|---|---|
| Sample ID | Zn | Pb | Tl | Fe | Mn | Zn | Pb | Tl | Fe | Mn |
| SFP 4 | 0.13 | 0.09 | 2.46 | 0.03 | 0.05 | 2.47 | 0.31 | 2.25 | 0.49 | 1.65 |
| SFP 11 | 0.95 | n.d. | 59.93 | 0.12 | 0.10 | 0.88 | n.d. | 4.55 | 2.17 | 3.57 |
| SFP 12 | 0.32 | n.d. | 2.12 | 0.09 | 0.10 | 0.75 | n.d. | 8.28 | 1.85 | 2.43 |
| SFP 13 | 0.10 | n.d. | 0.54 | 0.07 | 0.09 | 0.64 | n.d. | 5.16 | 2.21 | 2.04 |
| SFP 14 | 0.21 | n.d. | 6.27 | 0.07 | 0.06 | 0.49 | n.d. | 1.28 | 1.23 | 1.81 |
| SFP 15 | 0.12 | 0.03 | 1.92 | 0.00 | 0.05 | 0.57 | n.d. | 11.60 | 0.71 | 2.24 |
| SFP 16 | 0.14 | 0.08 | 12.33 | 0.03 | 0.15 | 1.35 | n.d. | 3.67 | 0.35 | 1.45 |
| SFP 17 | 0.05 | 0.03 | 1.10 | n.d. | 0.05 | 0.42 | 0.48 | 8.00 | 3.90 | 2.10 |
| SFP 18 | 0.07 | 0.06 | 19.80 | 0.03 | 0.06 | 0.44 | 0.13 | 4.62 | 0.91 | 1.49 |
| SFP 19 | 0.16 | 0.08 | 1.01 | 0.02 | 0.08 | 0.94 | 1.00 | 11.03 | 1.49 | 2.20 |
| SFP 20 | 0.03 | 0.06 | 0.19 | 0.01 | 0.04 | 0.21 | 0.03 | 3.06 | 0.19 | 1.00 |
| SFP 21 | 0.78 | n.d. | 4.24 | 0.01 | 0.03 | 1.76 | n.d. | 6.41 | 0.71 | 1.72 |

Journal of Environmental Management 186 (2017) 214–224

Contents lists available at ScienceDirect

Journal of Environmental Management

journal homepage: www.elsevier.com/locate/jenvman

Research article

# Bioaccumulation of thallium and other trace metals in *Biscutella laevigata* nearby a decommissioned zinc-lead mine (Northeastern Italian Alps)

Elena Pavoni [a], Elisa Petranich [a], Gianpiero Adami [b], Elena Baracchini [b], Matteo Crosera [b], Andrea Emili [a], Davide Lenaz [a], Pablo Higueras [c], Stefano Covelli [a, *]

[a] Department of Mathematics and Geosciences, University of Trieste, Italy
[b] Department of Chemical and Pharmaceutical Sciences, University of Trieste, Italy
[c] ICaA - University of Castilla La Mancha, Almadén, Ciudad Real, Spain

ARTICLE INFO

*Article history:*
Received 9 February 2016
Received in revised form
7 June 2016
Accepted 10 July 2016
Available online 30 July 2016

*Keywords:*
Trace metals
Thallium
*Biscutella laevigata*
Bioaccumulation
Soil
Mining activity

ABSTRACT

The mineral body exploited in Salafossa (Eastern Dolomites) was one of the largest lead/zinc-containing mineral deposits in Europe. Both metals were mainly present as sulphides (*sphalerite*, ZnS and *galena*, PbS). Mining activity started around 1550, but it was only around 1960 that the richest veins of the minerals were discovered. The mine closed in 1985, and concentrations of several trace metals, such as thallium (Tl), iron (Fe), manganese (Mn), lead (Pb) and zinc (Zn), were detected in the soils and plant samples (*Biscutella laevigata* L.) that were collected from eighteen sites selected outside the mine. *B. laevigata* is a *pseudometallophyta* species, and it often grows near mining areas where the soil's metal concentrations are significantly higher than those of soil with a natural geochemical background.

The total metal concentrations in the plant tissue (roots and leaves of *Biscutella laevigata*) and in the soil samples – both bulk-soil and the *B. laevigata* root system (rhizo-soil) – were determined through Inductively Coupled Plasma Optical Emission Spectrometry (ICP-OES). The metal extractability and leachability of the soil samples were estimated using soil extractions with DTPA (Diethylenetriaminepentaacetic acid). In addition, metal mobility caused by rainwater runoff was estimated by using a leaching test with a dilute solution of $H_2SO_4$ and $HNO_3$.

The results showed that metals were present in a chemical form available for uptake by the plants' roots. In fact, high concentrations of the metals were also found in the plant tissue (roots and leaves) of *B. laevigata*, and these concentrations were higher than those whose soils present natural geochemical background levels in the corresponding rhizo-soil. Thus, *B. laevigata* has shown a marked ability to bioaccumulate trace metals, especially Tl and, to a lesser extent, Zn, Pb, Fe and Mn, and it can influence metal mobility in the rhizo-soil.

To assess the uptake and translocation processes of the trace metals, resulting in their bioaccumulation, two different indices were calculated: the *enrichment factor in roots* (EFr), as the ratio between the metal concentration in belowground biomass and in the respective rhizo-soil, and the *translocation factor* (TF), as the ratio between the metal concentration in the leaves and the corresponding roots. For both indices, values > 1 denoted enrichment of the metal in the roots or its translocation to the upper tissues. The results showed that EFr and TF were considerably high only for Tl, reaching a maximum value of 60 for EFr and 11.6 for TF. Conversely, the other investigated metals did not show significant bioaccumulation (EFr < 1), and they showed TF > 1 only at a few sites.

Journal of Geochemical Exploration 188 (2018) 1–10

Contents lists available at ScienceDirect

Journal of Geochemical Exploration

journal homepage: www.elsevier.com/locate/gexplo

# Mobility and fate of Thallium and other potentially harmful elements in drainage waters from a decommissioned Zn-Pb mine (North-Eastern Italian Alps)

Elena Pavoni[a,b], Stefano Covelli[a,*], Gianpiero Adami[b], Elena Baracchini[b], Roberto Cattelan[c], Matteo Crosera[b], Pablo Higueras[d], Davide Lenaz[a], Elisa Petranich[a]

[a] Dipartimento di Matematica e Geoscienze, Università degli Studi di Trieste, Italy
[b] Dipartimento di Scienze Chimiche e Farmaceutiche, Università degli Studi di Trieste, Italy
[c] Veritas, Chemical Laboratory Venezia Rialto, Italy
[d] IGeA - Universidad de Castilla - La Mancha, Almadén, Ciudad Real, Spain

## ARTICLE INFO

*Keywords:*
Thallium
Potentially harmful elements
Mining activity
Mine drainage waters

## ABSTRACT

The potential impact of decommissioned mining areas on the quality of water resources is an issue of major concern for local communities. Acid mine drainage resulting from hydrolysis and oxidation of metal sulphides associated with mineral veins or mining wastes is often responsible for leaching large amounts of potentially harmful elements (PHEs) in solution, which can be dispersed into the surrounding environment and affect the quality of the recipient water bodies.

The aim of the present study was to investigate the geochemical properties of the mine drainage waters at the decommissioned Salafossa mine (North-Eastern Italian Alps), to highlight anomalous concentrations of PHEs outflowing from the currently flooded galleries and to elucidate their speciation.

In spite of the Zn-Pb sulphides still present in the body ore, there is no evidence of acid drainage waters from the mine galleries as a result of the buffering effect produced by carbonate host rocks. Due to their high mobility, however, Zn and Tl are present in solution mostly in ionic form. Conversely, the less mobile Pb, is preferably partitioned in the solid phase. Additionally, the oxidising conditions of the drainage waters also allow the precipitation of some PHEs (As, Cd, Pb, Tl, Zn) in the form of Fe-Mn oxy-hydroxides and carbonates, which accumulate at the bottom of the mine galleries as fine "sediments" or concretions. Drainage waters inside the mine were found to be highly enriched in Zn (up to 16 mg $L^{-1}$), Fe (up to 5 mg $L^{-1}$) and Tl (up to 260 μg $L^{-1}$). Their concentrations, however, are partially diluted in the mine due to a mixing with less mineralised waters before being discharged into the Piave River, the major tributary downstream from the mining area. Although drainage waters are still characterised by high concentrations of Tl (about 30 μg $L^{-1}$) at their outflow, dilution in the Piave River seems to be the only natural process mitigating the impact of PHEs within the drainage basin.

Journal of Geochemical Exploration 245 (2023) 107129

# Hydrogeochemistry of thallium and other potentially toxic elements in neutral mine drainage at the decommissioned Pb-Zn Raibl mine (Eastern Alps, Italy)

Nicolò Barago [a,*], Elena Pavoni [a], Federico Floreani [a,b], Matteo Crosera [c], Gianpiero Adami [c], Davide Lenaz [a], Stefano Covelli [a]

[a] Dipartimento di Matematica e Geoscienze, Università di Trieste, Via Weiss 2, 34128 Trieste, Italy
[b] Dipartimento di Scienze della Vita, Università di Trieste, Via Licio Giorgieri 5, 34127 Trieste, Italy
[c] Dipartimento di Scienze Chimiche e Farmaceutiche, Università di Trieste, Via Licio Giorgieri 1, 34127 Trieste, Italy

ARTICLE INFO

*Keywords:*
Thallium
Environmental impact
Carbonate-Hosted Pb-Zn
Tailings impoundments
Contamination
Long-term monitoring

ABSTRACT

Decommissioned mines represent a worldwide concern due to the potential long-term effects related to the dispersion of potentially toxic elements (PTEs) in the environment. In this study, 176 water samples were collected in the period 2018–2021 at the carbonate-hosted Pb-Zn Raibl mine which is affected by neutral mine drainage (NMD). The post-flotation tailings are the main source of PTEs (Zn, Pb and especially Tl) in the river drainage system. Compared to other dissolved PTEs (Zn, Pb, Cd), Tl was found to be more mobile, reaching concentrations up to 120 μg $L^{-1}$ in waters flowing in the tailings impoundments. Modelling results suggest that Tl is mainly present in the Tl(I) ionic and mobile form thus suggesting that relevant natural attenuation processes for this element are not expected in the investigated area. In contrast, Zn and Pb attenuation pathways appeared to be governed by pH-dependent speciation and sorption processes, whereas elevated Zn concentrations were likely also limited by hydrozincite precipitation. Metalloids such as As and Sb were almost entirely released into the slightly alkaline waters of the mine drainage system, which are generally characterised by longer residence time or standing waters whereas As and Sb concentrations were negligible in the tailings-seepage waters. However, intense rainy events may increase PTE concentrations of one order of magnitude, especially in the tailings impoundment groundwater as a result of a rise in the water table, and PTE total dissolved loads of three orders of magnitude, in the main stream during high flow events, thus representing the most critical factor in regulating the remobilisation and downward dispersion of PTEs in the river drainage system.

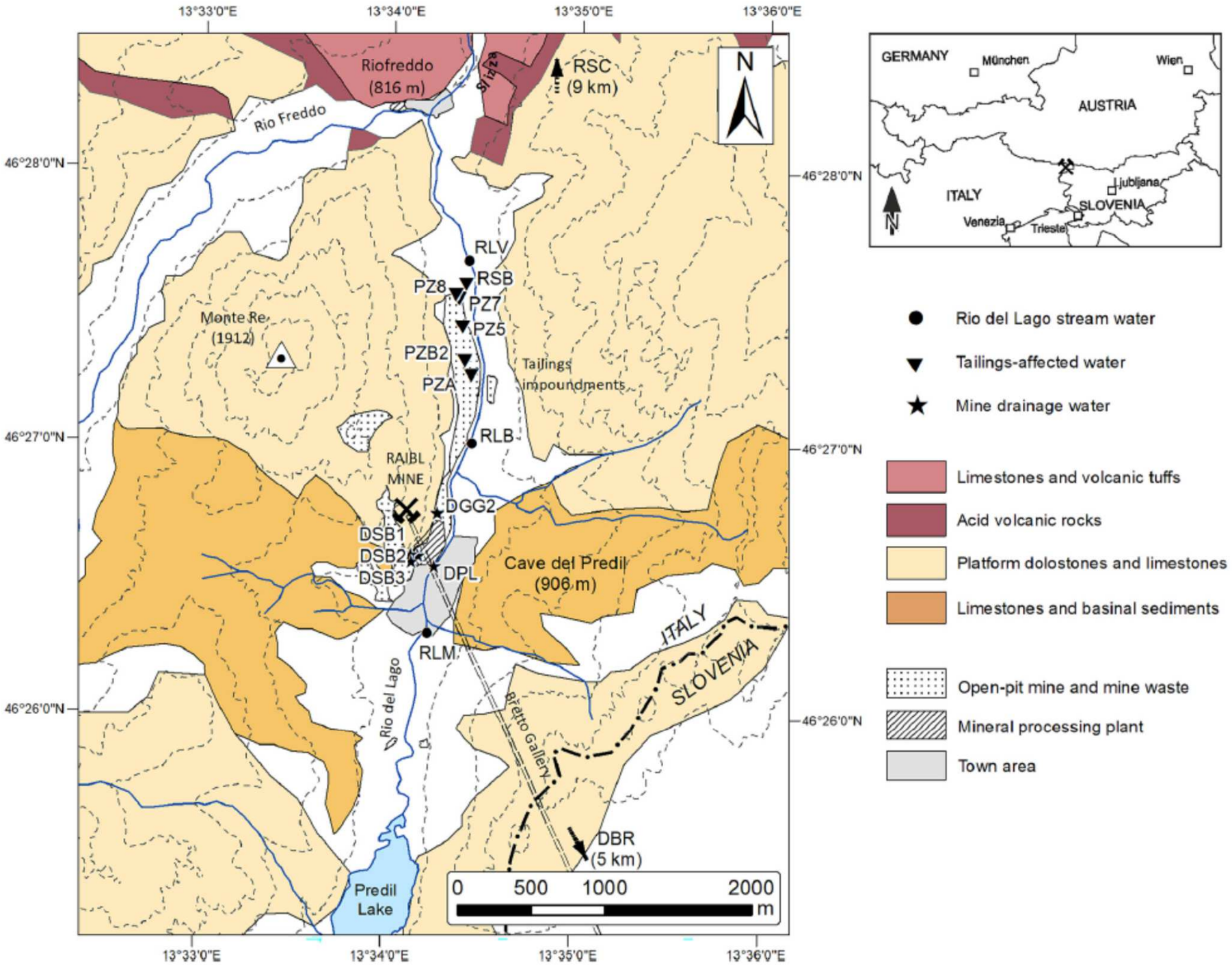
13°33'0"E
13°34'0"E
13°35'0"E
13°36'0"E
46°28'0"N
46°27'0"N
46°26'0"N
Riofreddo
(816 m)
Rio Freddo
Slizza
RSC
(9 km)
N
RLV
RSB
PZ8
PZ7
PZ5
PZB2
PZA
Monte Re
(1912)
Tailings
impoundments
RLB
RAIBL
MINE
DGG2
DSB1
DSB2
DSB3
DPL
Cave del Predil
(906 m)
RLM
Rio del Lago
Predil
Lake
Bretto Gallery
ITALY
SLOVENIA
DBR
(5 km)
0
500
1000
2000
m
GERMANY
München
Wien
AUSTRIA
ITALY
SLOVENIA
Ljubljana
Venezia
Trieste
Rio del Lago stream water
Tailings-affected water
Mine drainage water
Limestones and volcanic tuffs
Acid volcanic rocks
Platform dolostones and limestones
Limestones and basinal sediments
Open-pit mine and mine waste
Mineral processing plant
Town area

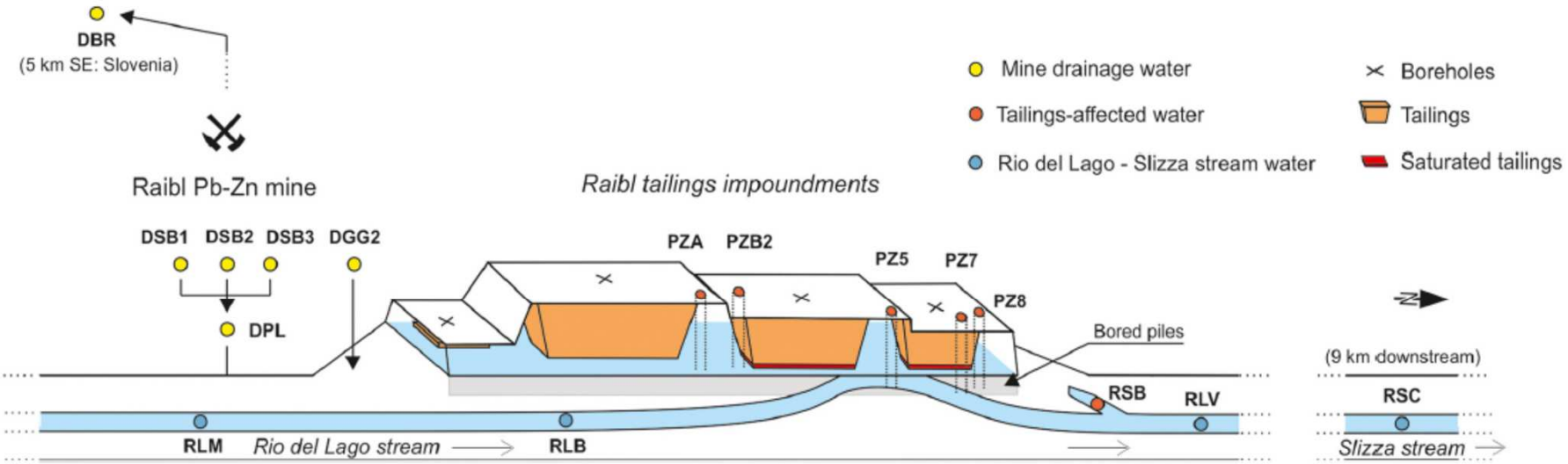


**Fig. 2.** Schematic representation of the decommissioned Raibl mining district showing the location of the monitored stations for different groups of water. The orange area represents the possible volumes of tailings stored in the ponds based on boreholes and geophysics (Barago et al., 2021).

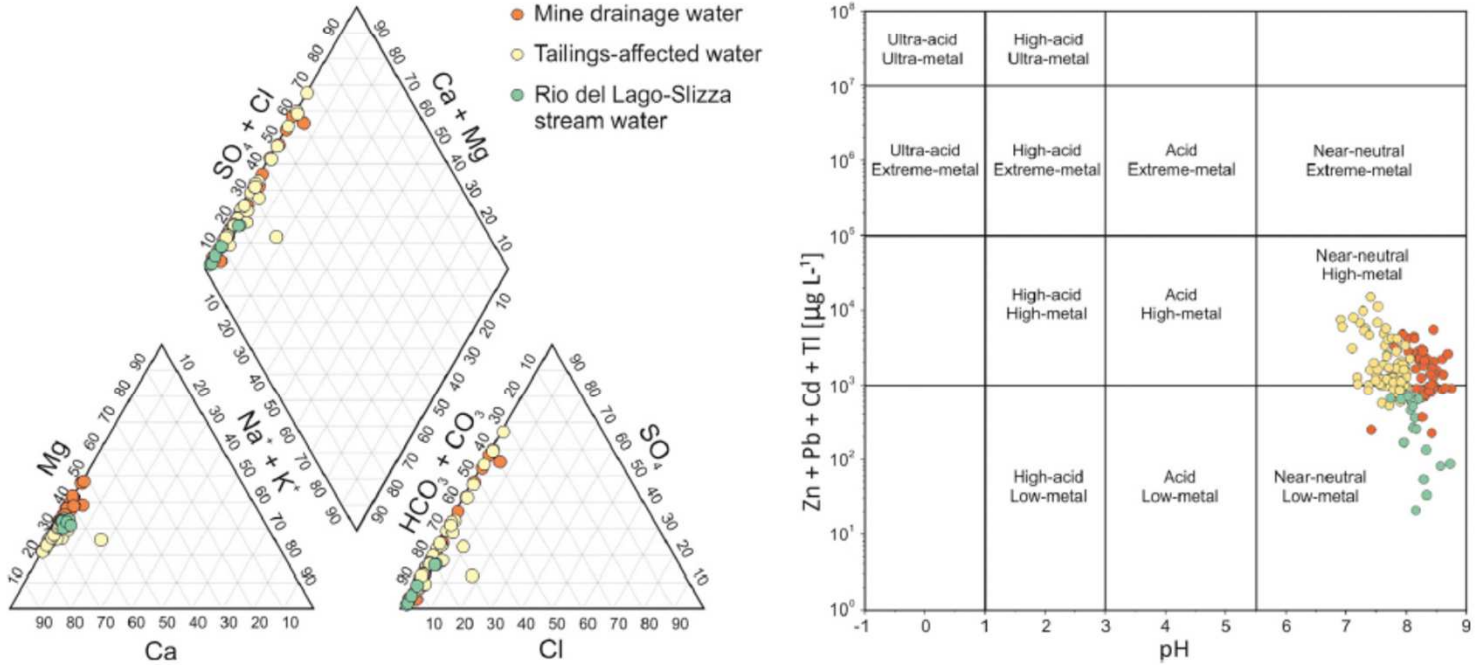


**Fig. 3.** Piper and modified Ficklin diagrams of the different groups of water collected at the decommissioned Raibl mining district.

**Table 3**
Average trace element concentrations (μg $L^{-1}$) in the different groups of water collected at the decommissioned Raibl mining district.

| | Mine drainage water (n = 54) | Tailings-affected water (n = 96) | Stream water (n = 26) |
|---|---|---|---|
| Zn | 1795 ± 1262 | 2349 ± 2519 | 341 ± 256 |
| Tl | 16.7 ± 14.1 | 38.3 ± 25.5 | 5.0 ± 5.8 |
| Pb | 11.5 ± 6.9 | 35.1 ± 17.0 | 16.9 ± 11.1 |
| Ba | 38.9 ± 17.5 | 56.2 ± 25.2 | 28.4 ± 16.3 |
| Cd | 1.26 ± 0.89 | 1.46 ± 2.38 | 0.28 ± 0.18 |
| As | 18.6 ± 27.0 | 1.4 ± 0.5 | 0.7 ± 0.3 |
| Sb | 2.40 ± 2.03 | 0.34 ± 0.20 | 0.16 ± 0.07 |
| Ge | 0.68 ± 0.35 | 0.42 ± 0.45 | 0.09 ± 0.07 |
| Fe | 10.03 ± 8.53 | 8.07 ± 8.79 | 6.41 ± 8.33 |
| Mn | 0.32 ± 0.20 | 0.28 ± 0.56 | 0.33 ± 0.59 |

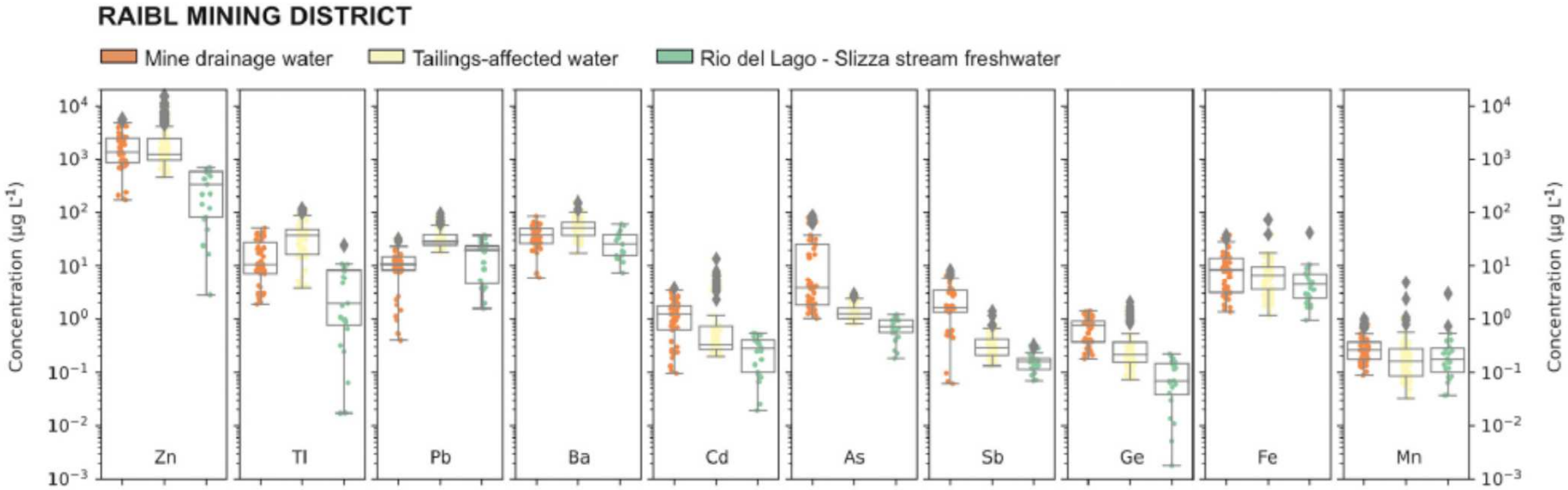


**Fig. 4.** Boxplot of potentially toxic trace element compositions in the mining district.

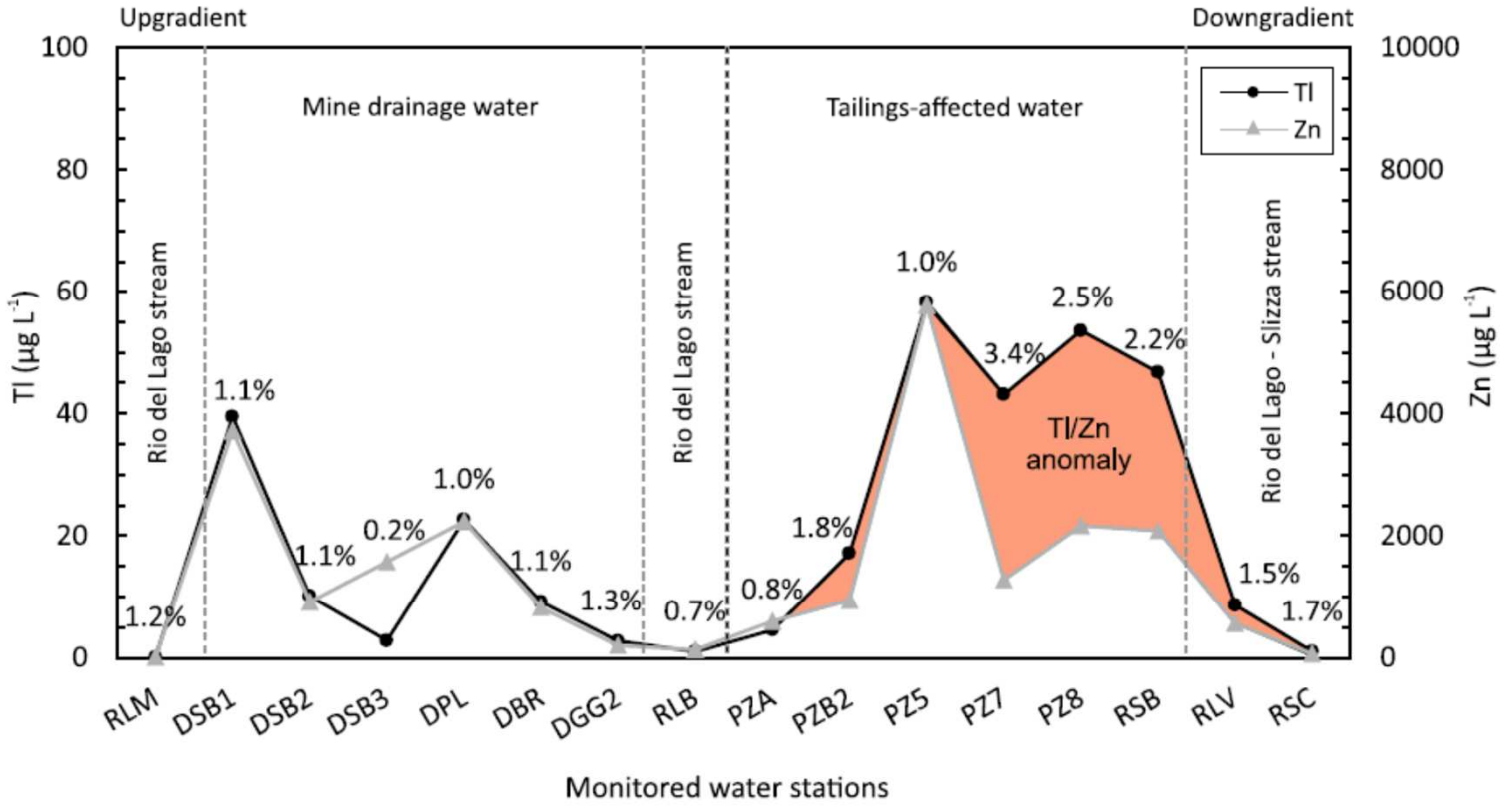


**Fig. 7.** Zinc and Tl concentrations in the different groups of waters collected upstream and downstream of the decommissioned Raibl mining district along the Rio del Lago Valley. The labels indicate Tl/Zn ratio (%).

Significantly high PTE concentrations persist in the drainage water system of the decommissioned Pb-Zn Raibl mining district despite almost 30 years of flushing after extraction and processing activities shut down. Differences in the geochemical signature were found in different monitored waters: the water affected by the leaching of tailings showed very high concentrations of Zn, Tl and Pb, whereas the waters draining the mine galleries were also enriched in As and, to a lesser extent, Sb. This could be explained by differences in the residence time and higher pH conditions of the water, which can promote the mobility of metalloids such as As due to desorption from HFOs. Anomalous high concentrations of Tl were found in waters affected by post-flotation tailings leaching, with Tl/Zn ratios 3–4 fold higher with respect to mine drainage and riverine waters. This anomaly of Tl was similarly observed with regard to other main PTEs, indicating that tailings are the main source of dissolved Tl in the water at the investigated decommissioned mining district.

Elevated Zn concentrations were also likely limited by hydrozincite precipitation. Results from this research also reveal that leaching processes involving tailings and the subsequent release and dispersion of PTEs are promoted during periods of intense rainfall and high flow river conditions. During such events the concentrations of metals in the groundwater found in tailings impoundments can be heavily increased by one order of magnitude, whereas the total dissolved load (TDL) in the main stream, the Rio del Lago, can be magnified by three orders of magnitude.

Environmental Science and Pollution Research (2023) 30:63754–63775
https://doi.org/10.1007/s11356-023-26629-7

# Environmental impact of potentially toxic elements on soils, sediments, waters, and air nearby an abandoned Hg-rich fahlore mine (Mt. Avanza, Carnic Alps, NE Italy)

Nicolò Barago[1] · Cristiano Mastroianni[1] · Elena Pavoni[1] · Federico Floreani[1] · Filippo Parisi[1] · Davide Lenaz[1] · Stefano Covelli[1]

Received: 16 September 2022 / Accepted: 20 March 2023 / Published online: 14 April 2023


## Abstract

The decommissioned fahlore Cu-Sb(-Ag) mine at Mt. Avanza (Carnic Alps, Italy) is a rare example of exploited ore deposits, as the tetrahedrite ($Cu_6[Cu_4(Fe,Zn)_2]Sb_4S_{13}$) is the main ore mineral found. This multi-compartmental geochemical characterisation approach provides one of the first case studies regarding the geochemical behaviour and fate of Hg, Sb, As, Cu, and other elements in solid and water matrices and of Hg in the atmosphere in an environment affected by the mining activity of a fahlore ore deposit. Elevated concentrations of the elements (Cu, Sb, As, Pb, Zn, Hg) associated with both (Zn-Hg)-tetrahedrite and to other minor ore minerals in mine wastes, soils, and stream sediments were observed. Concentrations in waters and stream sediments greatly decreased with increasing distance from the mining area and the $I_{geo}$ index values testify the highest levels of sediment contamination inside the mine area. Thallium and Ge were associated with the "lithogenic component" and not to sulfosalt/sulphide minerals. Although mine drainage water often slightly exceeded the national regulatory limits for Sb and As, with Sb being more mobile than As, the relatively low dissolved concentrations indicate a moderate stability of the tetrahedrite. The fate of Hg at the investigated fahlore mining district appeared similar to cinnabar mining sites around the world. Weak solubility but the potential evasion of gaseous elemental mercury (GEM) into the atmosphere also appear to be characteristics of Hg in fahlore ores. Although GEM concentrations are such that they do not present a pressing concern, real-time field surveys allowed for the easy identification of Hg sources, proving to be an effective, suitable high-resolution indirect approach for optimising soil sampling surveys and detecting mine wastes and mine adits.

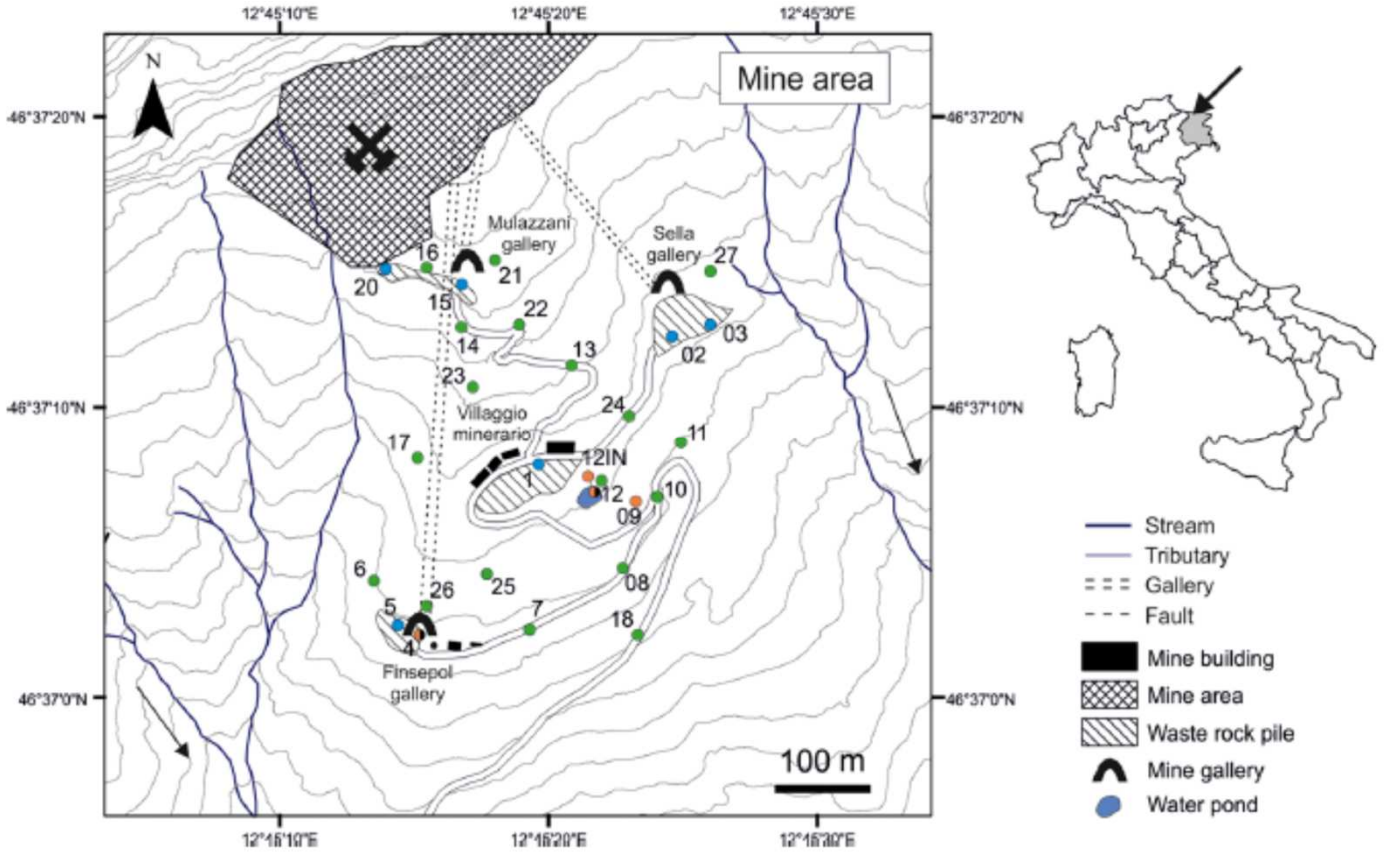
12°45'10"E
12°45'20"E
12°45'30"E
46°37'20"N
46°37'10"N
46°37'0"N
N
Mine area
Mulazzani gallery
Sella gallery
Villaggio minerario
Finsepol gallery
100 m
Stream
Tributary
Gallery
Fault
Mine building
Mine area
Waste rock pile
Mine gallery
Water pond


**Fig. 2** **a** Outcrop of alteration supergene minerals related to the tetrahedrite Cu-Sb-(Ag) mineralisation "Pietra Verde", **b** mining village of the Mt. Avanza mine ("Villaggio minerario"), **c** Finsepol gallery, **d** Avanza valley and Avanza stream

**Table 2** Summary of the concentrations (min-max) of the main metals and metalloids in the environmental matrices

| | Type (*n* samples) | As | Cu | Hg | Sb | Pb | Zn |
|---|---|---|---|---|---|---|---|
| | | *mg/kg* | *mg/kg* | *mg/kg* | *mg/kg* | *mg/kg* | *mg/kg* |
| **Solid** | Waste rock pile (6) | 8.20-654 | 31.3-4019 | 1.42-473 | 5.00-1049 | 19.4-397 | 20.3-553 |
| | Soil (18) | 12.1-162 | 10.1-1557 | 0.21-132 | 2.74-153 | 26.4-1216 | 62.0-1204 |
| | Sediment (12) | 12.9-212 | 14.0-242 | 0.04-9.15 | 1.64-28.0 | 14.7-78.8 | 57.1-171 |
| | | *µg/L* | *µg/L* | *ng/L* | *µg/L* | *µg/L* | *µg/L* |
| **Water** | Mine drainage (11) | 0.87-14.8 | 0.29-8.28 | 2.41-13.2 | 4.33-20.3 | < LOD-1.02 | < LOD-11.0 |
| | Tributaries (5) | 0.18-3.89 | 0.12-0.41 | 1.81-10.2 | 0.19-1.59 | < LOD | < LOD-1.90 |
| | Main river (5) | 0.60-2.98 | <LOD-1.08 | 1.17-6.49 | 0.30-1.16 | < LOD-0.72 | < LOD-4.30 |
| | | | | *ng/m³* | | | |
| **Gas** | Mine area (1222) | n.d. | n.d. | < LOD-25.4 | n.d. | n.d. | n.d. |
| | Avanza valley [a] (344) | n.d. | n.d. | < LOD-13.7 | n.d. | n.d. | n.d. |
| | Rural area [b] (134) | n.d. | n.d. | < LOD-4.50 | n.d. | n.d. | n.d. |

[a]Between the mine and the downstream rural area

[b]The villages of Pierabech and Forni Avoltri (Fig. 1)

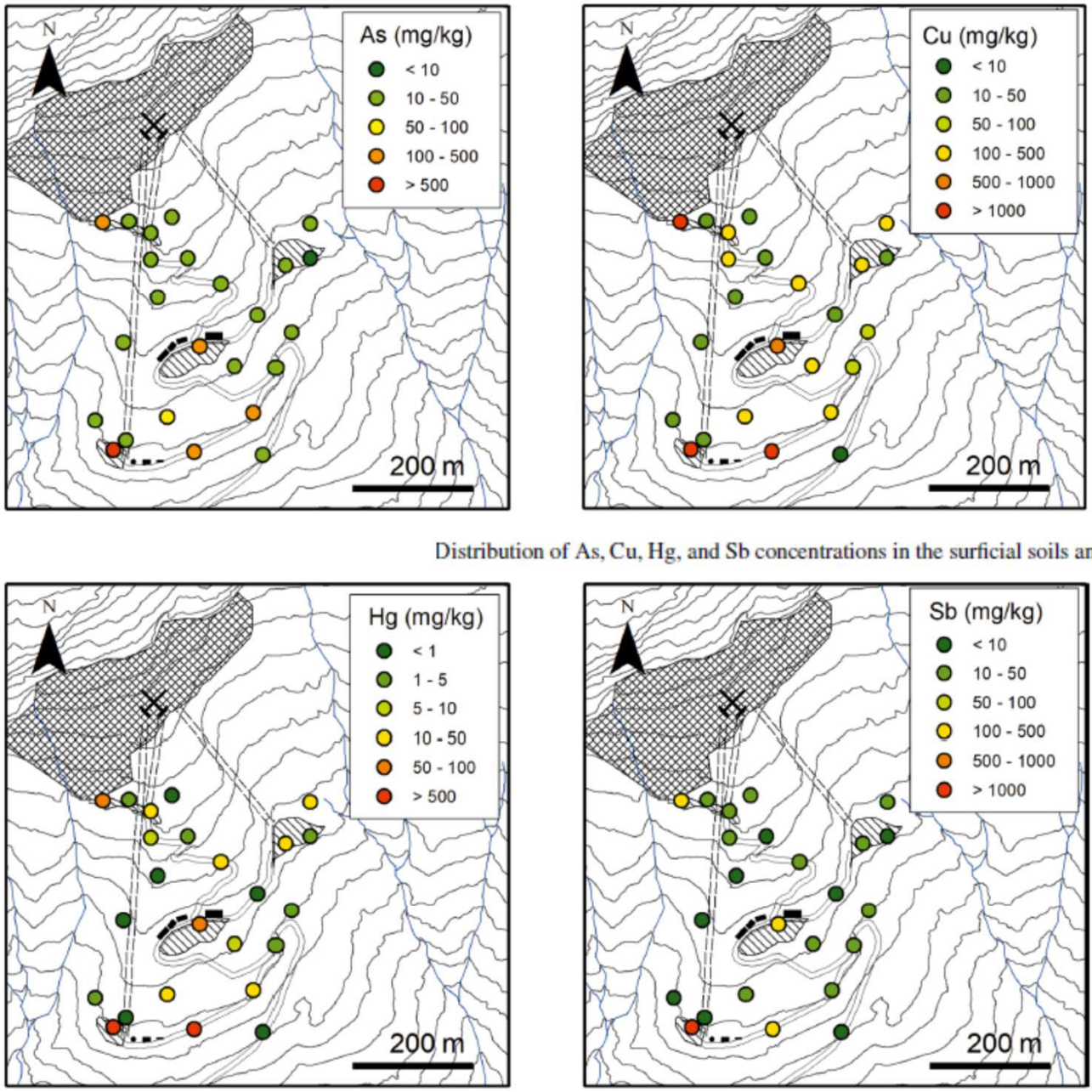


Distribution of As, Cu, Hg, and Sb concentrations in the surficial soils and waste rocks of the Mt. Avanza mining area

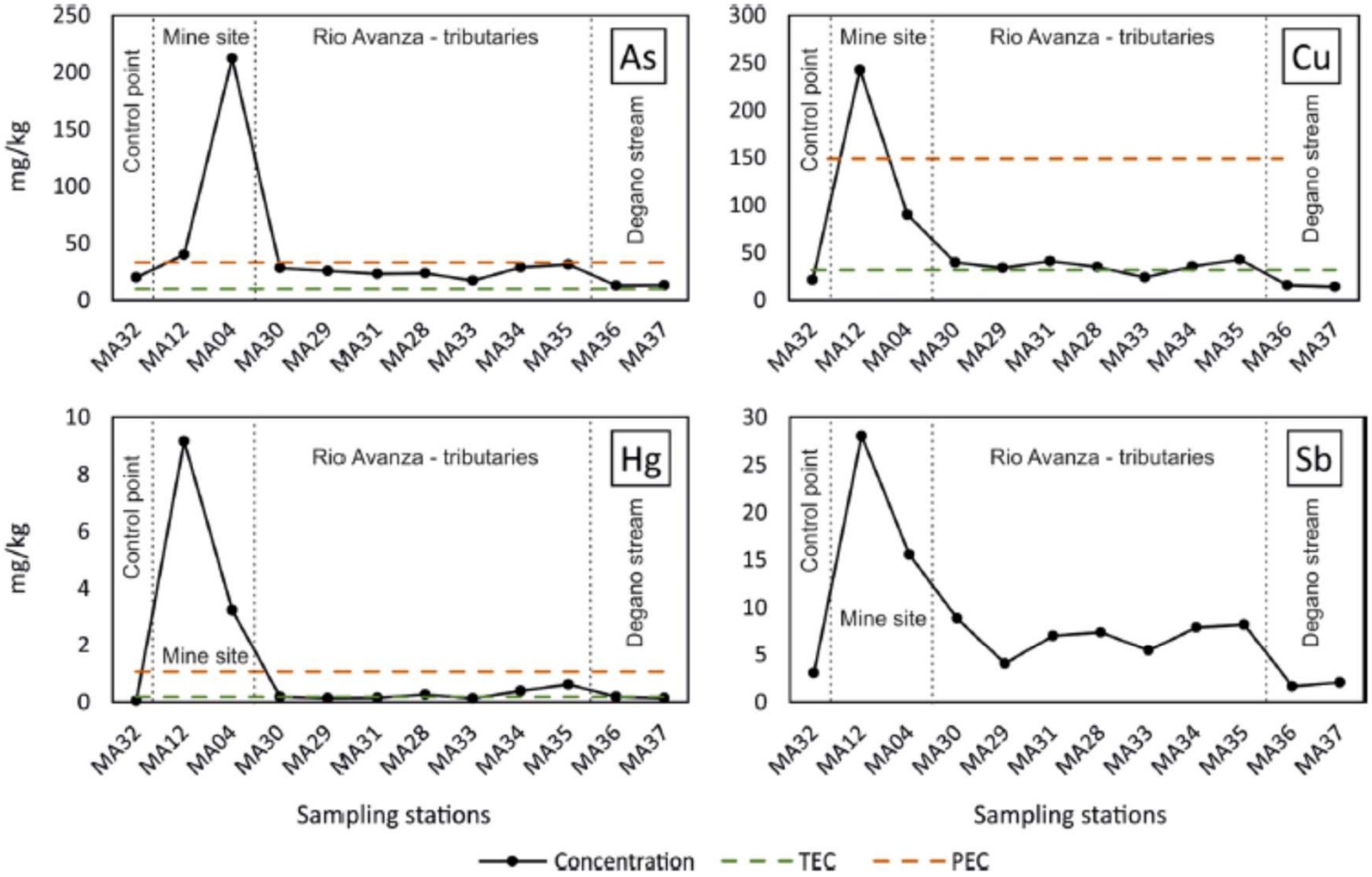


**Fig. 6** Concentrations of As, Cu, Hg, and Sb of stream sediments collected at the historic mining district of Mt. Avanza. Threshold effect concentration (TEC) and probable effect concentrations (PEC) from MacDonald et al. (2000)

**Table 3** Geoaccumulation index (Igeo) (Müller 1969) for stream sediments of the Rio del Lago-Slizza stream sediments. Igeo > 5 are highlighted in bold. MA32 was selected as "control sample".

| Type | Name | As | Cd | Cr | Cu | Fe | Ge | Hg | Mn | Mo | Ni | Pb | Sb | Tl | Zn |
|---|---|---|---|---|---|---|---|---|---|---|---|---|---|---|---|
| | *Concentration (mg/kg)* | | | | | | | | | | | | | | |
| | MA32 | 19.8 | 0.15 | 62.3 | 21.2 | 36890 | 1.84 | 0.04 | 525 | 1.22 | 32.0 | 21.9 | 3.06 | 0.74 | 86.3 |
| | $I_{geo}$ | | | | | | | | | | | | | | |
| Mine area | MA12 | -0.1 | 1.4 | -1.1 | **2.9** | -1.3 | -1.2 | **7.3** | -1.2 | -2.1 | -1.0 | 1.1 | **2.9** | -1.1 | 0.0 |
| Mine area | MA04 | **2.8** | 0.9 | -0.7 | 1.5 | -0.9 | -0.4 | **5.8** | -0.7 | -0.5 | -0.3 | 0.9 | 1.8 | -0.6 | 0.3 |
| Main stream | MA28 | -0.3 | 1.0 | -0.1 | 0.1 | -0.1 | -0.6 | **2.2** | -0.4 | -0.5 | -0.2 | -0.2 | 0.7 | -0.6 | 0.2 |
| Main stream | MA34 | 0.0 | 1.2 | -0.1 | 0.2 | -0.3 | 0.0 | **2.7** | -0.6 | -0.7 | -0.3 | 0.4 | 0.8 | -0.3 | 0.1 |
| Main stream | MA35 | 0.1 | 1.5 | -0.2 | 0.4 | -0.3 | -0.7 | **3.4** | -0.2 | -0.1 | -0.4 | 0.7 | 0.8 | -0.4 | 0.1 |
| Main stream | MA37 | -1.2 | -1.2 | -0.9 | -1.2 | -0.2 | -0.4 | 1.1 | -1.3 | -0.6 | -1.1 | -1.1 | -1.2 | -1.2 | -1.2 |
| Tributaries | MA30 | -0.1 | 1.4 | 0.1 | 0.3 | -0.5 | -0.8 | 1.6 | -0.6 | -0.9 | 0.0 | 0.1 | 1.0 | -0.3 | 0.4 |
| Tributaries | MA29 | -0.2 | -0.5 | -0.6 | 0.1 | -0.4 | -0.6 | 1.1 | -0.6 | -1.6 | -0.7 | 0.0 | -0.2 | -0.1 | -0.1 |
| Tributaries | MA31 | -0.4 | 1.1 | -0.1 | 0.4 | -0.5 | -0.6 | 1.3 | -0.7 | -0.8 | -0.2 | 0.8 | 0.6 | -0.6 | 0.2 |
| Tributaries | MA33 | -0.8 | -1.0 | -0.6 | -0.4 | -1.3 | -0.9 | 1.0 | -0.7 | -0.9 | -0.6 | -0.4 | 0.2 | -0.7 | -0.5 |
| Tributaries | MA36 | -1.2 | -0.9 | -0.8 | -1.0 | -1.4 | -0.9 | 1.6 | -1.1 | -0.5 | -0.5 | -1.2 | -1.5 | -1.1 | -1.1 |

| Value | Class | Contamination level |
|---|---|---|
| Igeo < 0 | 1 | Uncontaminated |
| $0 < I_{geo} \leq 1$ | 2 | Uncontaminated to moderately contaminated |
| $1 < I_{geo} \leq 2$ | 3 | Moderately contaminated |
| $2 < I_{geo} \leq 3$ | 4 | Moderately to heavily contaminated |
| $3 < I_{geo} \leq 4$ | 5 | Heavily contaminated |
| $4 < I_{geo} \leq 5$ | 6 | Heavily to extremely contaminated |
| $5 < I_{geo} \leq 6$ | 7 | Extremely contaminated |

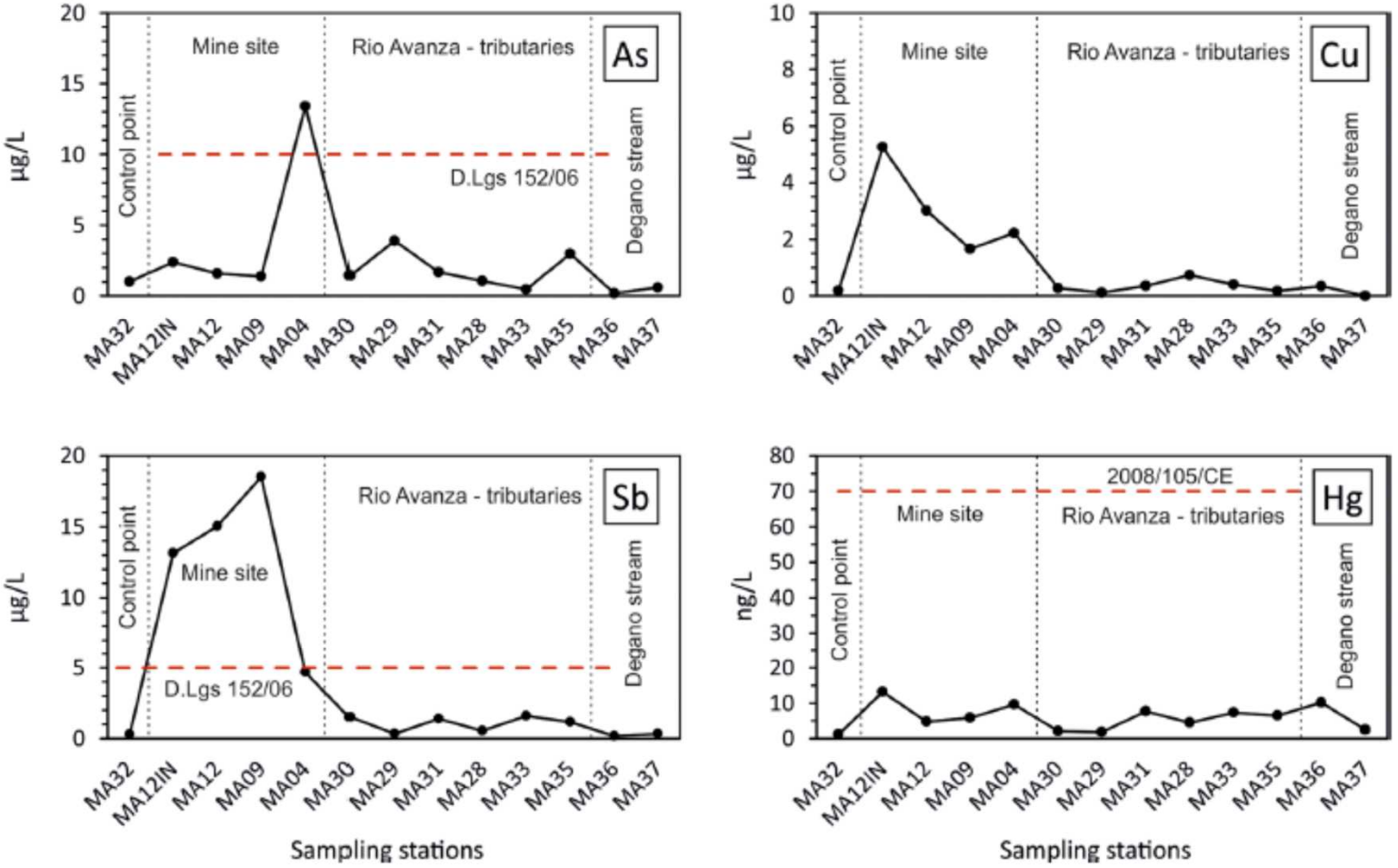


**Fig. 8** Concentrations of As, Cu, Hg, and Sb in water collected at the historic mining district of Mt. Avanza. D.Lgs. 152/06: Italian reference legislation for groundwater quality. 2008/105/CE European water quality standard

The geochemical signature of the past mining activity at the Cu-Sb(-Ag) Mt. Avanza ore deposit was evidenced by notable concentrations of the elements associated with the (Hg-Zn)-rich tetrahedrite in mine wastes, soils, and stream sediments (max: Cu = 4019 mg/kg, Sb = 1049 mg/ kg, Pb = 1216 mg/kg, Zn = 1204 mg/kg, As = 654 mg/kg and Hg = 473 mg/kg). Results from this research suggest that extraction activities as well as the by-products employed in the constructions of roads and mine facilities contribute to a heterogeneous distribution of PTE concentrations in the soil matrix. Conversely, notable amounts of PTEs in the stream sediments appeared to be restricted to the mining area as shown by the general decrease in the PTE concentrations with increasing distance from the source area. This was confirmed by the Igeo index values which were found to be significantly high inside the mine area.

Regarding solid-water interactions, the water draining the mining district belonged to a “neutral mine drainage” as the result of pH buffering effects due to dissolution of the Devonian carbonate host rocks, promoting the release of Sb, which was found to be generally more mobile than As in solution. Although mine drainages often exceeded the national regulatory limits for Sb and As, relatively low dissolved concentrations of the main metal(loid)s were observed, suggesting the moderate stability of the tetrahedrite and other minor ore-bearing minerals as well as the occurrence of natural attenuation processes along the river system, most likely due to dilution, (co-)precipitation, and potential sorption processes.



Therefore, it appears that the Mt. Avanza mine is not a relevant source of contamination for the area.